A PM10 chemically characterized nation-wide dataset for Italy. Geographical influence on urban air pollution and source apportionment

Adriana Pietrodangelo [a],[*],[1], Maria Chiara Bove [b],[1], Alice Corina Forello [c],[1], Federica Crova [c],[1], Alessandro Bigi [d], Erika Brattich [e], Angelo Riccio [f], Silvia Becagli [g], Stefano Bertinetti [h], Giulia Calzolai [i], Silvia Canepari [j], David Cappelletti [k], Maria Catrambone [l], Daniela Cesari [m], Cristina Colombi [n], Daniele Contini [m], Eleonora Cuccia [n], Gianluigi De Gennaro [o], Alessandra Genga [p], Pierina Ielpo [m], Franco Lucarelli [q], Mery Malandrino [h], Mauro Masiol [r], Dario Massabò [s], Cinzia Perrino [a], Paolo Prati [s], Tiziana Siciliano [t], Laura Tositti [u], Elisa Venturini [v], Roberta Vecchi [c]

[a] C.N.R. Institute of Atmospheric Pollution Research, Monterotondo St., Rome 00015, Italy
[b] Ligurian Regional Agency for Environmental Protection (ARPAL), Genoa 16149, Italy
[c] Department of Physics, University of Milan and INFN-Milan, 20133 Milan, Italy
[d] Department of Engineering "Enzo Ferrari", University of Modena and Reggio Emilia, Modena 41125, Italy
[e] Department of Physics and Astronomy "Augusto Righi", University of Bologna, Bologna 40126, Italy
[f] Department of Science and Technology, University of Naples Parthenope, Naples 80143, Italy
[g] Department of Chemistry "Ugo Schiff", University of Florence, Sesto Fiorentino, Florence 50019, Italy
[h] Department of Chemistry, University of Turin, 10125 Turin, Italy
[i] National Institute of Nuclear Physics (INFN), Sesto Fiorentino, Florence 50019, Italy
[j] Department of Environmental Biology, Sapienza University of Rome, 00185 Rome, Italy
[k] Department of Chemistry, Biology and Biotechnology, University of Perugia, 06123 Perugia, Italy
[l] C.N.R. Institute of Heritage Science, Milan 20125, Italy
[m] C.N.R. Institute of Atmospheric Sciences and Climate, ISAC-CNR, Lecce 73100, Italy
[n] Regional Agency for Environmental Protection of Lombardy (ARPA Lombardia), Milan 20124, Italy
[o] Department of Biology, University of Bari "Aldo Moro", Bari 70121, Italy
[p] Department of Biological and Environmental Sciences and Technologies DISTeBA, University of Salento, Lecce 73100, Italy
[q] Department of Physics and Astrophysics, University of Florence and INFN-Florence, Sesto Fiorentino, Florence, 50019, Italy
[r] Department of Environmental Science, Informatics and Statistics, University Ca' Foscari, 30172 Mestre-Venezia, Italy
[s] Department of Physics, University of Genoa and INFN-Genoa, 16146 Genoa, Italy
[t] Department of Mathematics and Physics "Ennio De Giorgi", University of Salento, Lecce 73100, Italy
[u] Department of Chemistry "Giacomo Ciamician", University of Bologna, Bologna, 40126, Italy
[v] Department of Industrial Chemistry "Toso Montanari", University of Bologna, Bologna 40126, Italy

* Corresponding author.
  E-mail address: pietrodangelo@iia.cnr.it (A. Pietrodangelo).
[1] Shared first authorship.

HIGHLIGHTS

- A methodology to build a nation-wide PM_{10} dataset is provided.
- An unprecedented reference repository of PM_{10} composition for Italy is obtained.
- The dataset with atypical time resolution is successfully exploited as input for PMF.
- Country-scale chemical profiles retrieved by PMF contribute to profiles repositories.
- The approach can be employed with datasets typically available in the AQ networks.

GRAPHICAL ABSTRACT
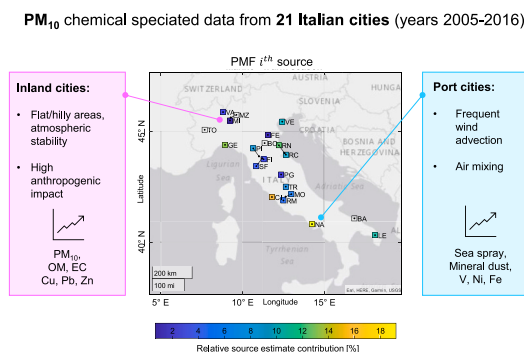
PM_{10} chemical speciated data from **21 Italian cities** (years 2005-2016)

ABSTRACT

Urban textures of the Italian cities are peculiarly shaped by the local geography generating similarities among cities placed in different regions but comparable topographical districts. This suggested the following scientific question: can different topographies generate significant differences on the PM_{10} chemical composition at Italian urban sites that share similar geography despite being in different regions? To investigate whether such communalities can be found and are applicable at Country-scale, we propose here a novel methodological approach. A dataset comprising season-averages of PM_{10} mass concentration and chemical composition data was built, covering the decade 2005–2016 and referring to urban sites only (21 cities). Statistical analyses, estimation of missing data, identification of latent clusters and source apportionment modeling by Positive Matrix Factorization (PMF) were performed on this unique dataset. The first original result is the demonstration that a dataset with atypical time resolution can be successfully exploited as an input matrix for PMF obtaining Country-scale representative chemical profiles, whose physical consistency has been assessed by different tests of modeling performance.

Secondly, this dataset can be considered a reference repository of season averages of chemical species over the Italian territory and the chemical profiles obtained by PMF for urban Italian agglomerations could contribute to emission repositories.

These findings indicate that our approach is powerful, and it could be further employed with datasets typically available in the air pollution monitoring networks.

1. Introduction

It is widely recognized that the chemical composition of airborne particulate matter (PM) affects a number of human and environmental key aspects like health, climate changes, ecosystems, and cultural heritage (see e.g., Krumbein and Gorbushina, 2009; Grau-Bové and Strlič, 2013; Amato-Lourenco et al., 2017; Kinney, 2018; Park et al., 2018; Corsini et al., 2019; Fang et al., 2019; Tuet et al., 2019; Bellouin et al., 2020; Arias et al., 2021; Vidović et al., 2022; and references therein).

The variability in PM composition is tuned by the site-related physical system, e.g. activity of point and diffuse sources, local and synoptic meteorology, mixing efficiency of the lower troposphere, strength of gas-to-particle conversion processes forming secondary aerosol, seasonal frequency of advection episodes (Belis et al., 2019). Moreover, peculiar orography and geography of the investigated area, such as large plains or the proximity to mountains and/or large water bodies, may univocally impact one site with respect to others pertaining to the same classification, especially as for the atmospheric dispersion of pollutants and the frequency of advection episodes. In Italy, extremely different geographical areas, like the Po plain, the extended coastline facing the Mediterranean Sea, and the mountain valleys of Alps and Apennines extending along the peninsula, closely alternate within a narrow territory, being the seventh largest EU country (Eurostat, 2022a) by total surface area, but having average width lower than 500 km only (Isprambiente, 2011).

More details about the features of these territories are reported in the

Supplementary Material, Section S1. Many Italian regions include more different geographical systems. Therefore, the specific location of cities in the same regional entity is an important feature that can drive different efficiencies in pollution. Extended research has been carried out in Italy in the last decades focusing on the chemical speciation and source apportionment of PM at city level and carried out in the frame of multi-city/multi-year projects at regional scale (Perrino et al., 2008; Carbone et al., 2010; Bove et al., 2014; Sandrini et al., 2014; Masiol et al., 2020; Cesari et al., 2021; ARPA Umbria, 2016; PREPAIR *Life15* Project). Many urban sites have been individually characterized by main factors responsible for local air pollution, including site-related geography and topography (Moroni et al., 2012; Cesari et al., 2014; Amato et al., 2016; Massimi et al., 2017; Merico et al., 2021; Tositti et al., 2022; Daellenbach et al., 2023).

It is noteworthy that a nation-wide linkage among cities influenced by the same geographical system, beyond their regional boundaries, is still missing, whereas it would support identifying mitigation measures more targeted at specific city-geography features.

To fill this gap, in this work we propose a novel methodology based on the estimation of missing data and the identification of latent clusters followed by receptor modeling, to investigate if different topographies are able to generate significant differences on the PM chemical composition at Italian urban sites that share similar geography despite being in different regions and if such communalities can be applicable at Country-scale. In details, the novel methodology is aimed at:

1. Identifying the main city-geography relationships, considered for city size (large or medium agglomerations) and geographical-topographical system (Po plain, other inland areas, coastline with/without commercial port), with respect to the variability of urban PM_{10} composition across Italy;
2. assessing if PM_{10} compositional profiles representative of different city-geography relationships show significant differences among each other;
3. exploring the potential of the dataset as a reference repository of season-averages of PM_{10} chemical species by city-geography, particularly for trace elements scarcely available from routine measurements, to be employed in cases where replacement of missing data is required;
4. evaluating the suitability of employing average values of PM composition as input for source apportionment modeling, e.g., by Positive Matrix Factorization (PMF).

To investigate such points, the Working Group on Sources and Environmental Impact of Aerosol of the Italian Aerosol Society (IAS. https://www.iasaerosol.it/) collected PM_{10} data of mass concentration and chemical composition by voluntary contribution of many research groups from Italian universities, research institutions, and regional environmental protection agencies.

A dataset (hereafter called IAS dataset of PM_{10}) has been built, covering the 2005–2016 period and comprising season-averaged chemical speciation data directly provided by the participating institutions; chemical composition PM_{10} data (both major species and trace elements) refer to urban sites of large or medium cities in the Po plain, inland areas or coastlines, across the Italian territory.

To the authors' knowledge, there are no previous literature works documenting latent clustering related to aerosol chemical speciation data and PMF applications to datasets with such time resolution and spatialization as extensively reported in this work.

2. Materials and methods

2.1. Dataset description

An array of average PM_{10} mass and its chemical composition was compiled, providing 110 cases by 40 chemical variables in the 2005–2016 period. In this work, a case in the dataset is defined as the average values of PM_{10} mass and composition referring to one site for one season and one year; each different combination of site-season-year identifies univocally a different case, as well as different sites in the same city. The cases were grouped by the season(s) (winter (W), spring (S), summer (SU), fall (F)) indicated for each average value by the contributing authors and ranked from less to more recent years within each season; each case is thus identified by the combination of season abbreviation and ranking number within the season group. While the PM_{10} mass concentration was provided for all cases, a few species (i.e., PAHs, levoglucosan, and some trace elements) were poorly available. Minimum data coverage for any chemical variable, to be considered for the goal of subsequent investigations, was set to 60 % of total cases.

Locations included in this dataset reflect siting criteria of the urban background type, under the 2008/50/EC Ambient Air Quality Directive (AAQD) requirements (Nagl et al., 2019). The sites are referred to 21 urban agglomerations of the Italian territory, namely (from North to South): Torino, Varese, Monza, Milano, Venezia, Ferrara, Bologna,
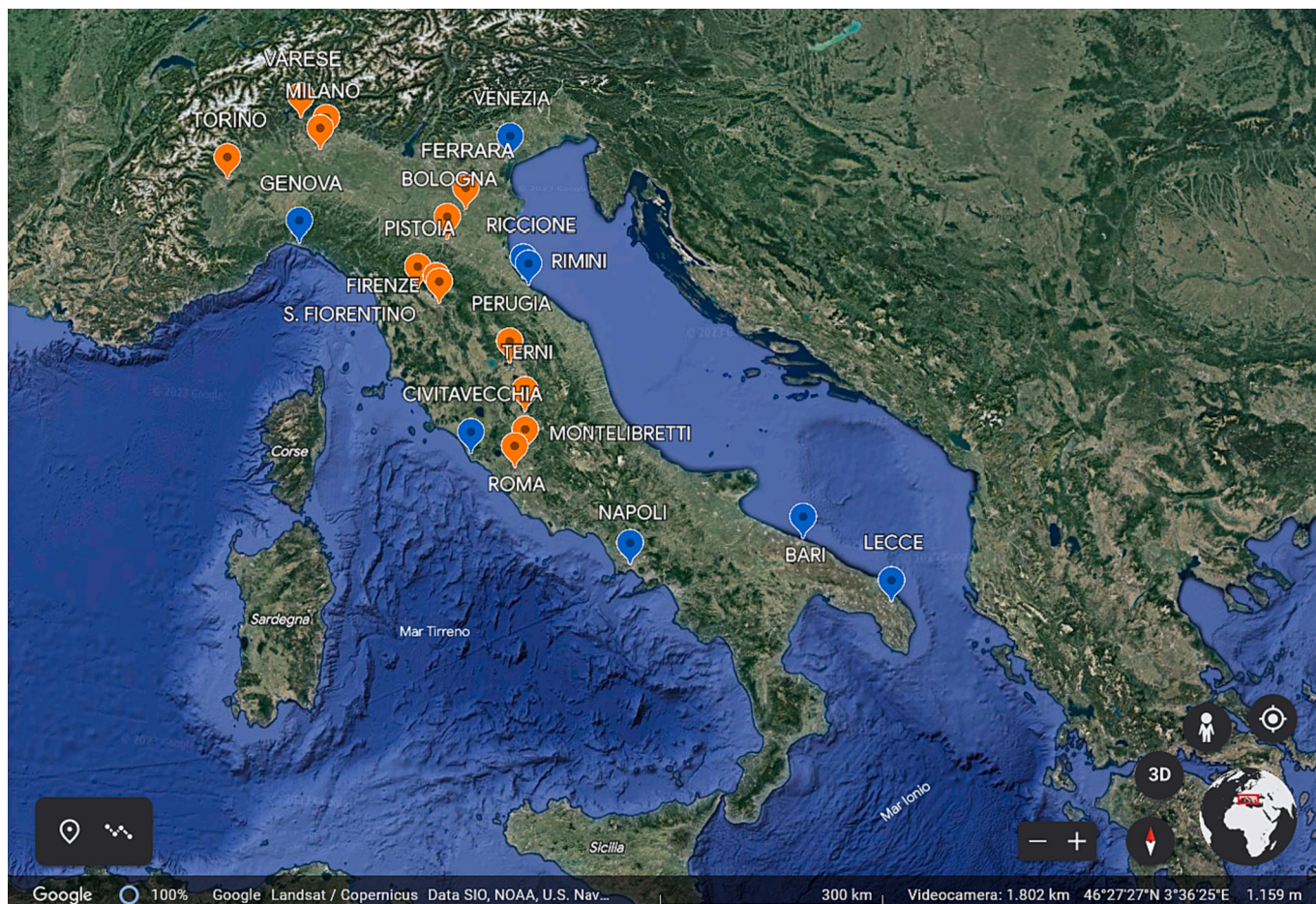

Fig. 1. Map of the cities of this study. Placemarks color indicates inland (orange) or coastal (blue) cities.

Genova, Rimini, Riccione, Pistoia, Sesto Fiorentino, Firenze, Perugia, Terni, Civitavecchia, Montelibretti, Roma, Napoli, Bari, Lecce (Fig. 1). A short description of the locations (geography, landscape, urban context, population density) and of cases (site name, coordinates, sampling years/seasons) is reported in Table 1 and more details can be found in the related literature.

First, a preliminary survey was carried out on data availability; an ad-hoc prepared questionnaire was supplied to this aim. Then, calls for data submission were launched: participants were asked to compile a form with chemical speciation data available from previous measurements and field studies, on a voluntary basis. Time resolution established for data of both PM_{10} mass concentration and chemical composition is season average and standard deviation, referring to an individual site by year and including at least two analytical determinations among inorganic ions, major elements, EC, OC, TC, levoglucosan, minor-trace elements, PAHs, in addition to PM_{10} mass. Participants were requested to directly provide season averages calculated by their respective laboratories, instead of data series. By this way, pre-existing awareness of site peculiarities was intrinsically included in calculation by the responsible for data, thus enhancing both the site-related representativeness and the overall signal-to-noise ratio of the chemical information. All average values of PM_{10} mass and chemical composition of the dataset refer to 24-h time resolution, corresponding to that of sample collection for most field campaigns where data originate from. In a few cases, sampling time was lower than 24-h; these data were thus aggregated to 24-h. A summary on the sampling techniques and the analytical methods can be found in the Supplementary Material (Section S2) and details on the experimental design of the original research studies contributing to this dataset can be found in references reported in Table 1 and in the Supplementary Material, Section S2.

2.2. Quality assurance and quality control

Average values of chemical composition and PM_{10} mass reported in this dataset have heterogeneous origins, differing - with respect to the aims of the original field study - for sampling period, duration and year, laboratory protocols of sample pre-treatment, and analytical determinations. Therefore, the physical soundness of the overall data array is less predictable than considering arrays of measured data obtained by ad-hoc sampling and experimental design. Physical consistency was thus investigated by three different modalities: within a single case, within individual species (variability range and seasonal behaviour), and for species-to-species relationships compared to those expected at urban sites. Results of data quality control were used to address the issue of missing data.

First, the within-case consistency was checked. Mass contributions of aerosol macro-components (mineral dust, sea spray, secondary inorganic aerosol, organic matter, and fossil fuel combustion) were calculated by empirical mass closure (Perrino et al., 2014) using the mean values provided by case; the sum of estimated mass contributions was matched against the corresponding mean value of measured PM_{10} mass. Concerning the assessment of individual chemical variables, ammonium, nitrate and sulphate ions were checked for soundness with the season evolution commonly expected for secondary inorganic aerosol; prior to this, total sulphate was empirically apportioned to sea-salt and non-sea salt fractions (Chow et al., 2015). Further, in a number of cases in the dataset both ion and total determinations of element were provided, in particular for Na (Na^+), Mg (Mg^{2+}), K (K^+), Ca (Ca^{2+}), and S (SO_4^-). Ordinary least square regression analysis (OLS) was thus employed to control that the relationship between the ion and the total content was consistent.

Consistency checks across the dataset structure included the following: mass contributions obtained by empirical mass closure were ranked by decreasing values, to assess the coherence of trends with respect to size of urban agglomeration, season and geographical location; OLS regressions between different chemical variables were

evaluated with respect to variability typical of urban sites; selected diagnostic ratios were compared to those of suitable literature source profiles; chemical equivalents of anions and cations were calculated, and ion balance analysis was carried out by anions-to-cations regression (Fig. S1).

As previously stated, with the purpose of selecting the chemical variables to be subjected to further investigations, a 60 % threshold of minimum data coverage was imposed. This led to a final data matrix with a 23×110 size. Nevertheless, missing values also affected variables which passed this selection, due to the different origins of data. In this work, the need of having a dataset with no missing values is driven by the purpose of exploring its potential both as reference repository of city-geography specific season averages of chemical species in PM_{10}, and as unconventional input dataset for PMF analyses, as done here for the first time. For Na, K and Ca, the OLS analysis between total and ion determination (as previously reported) shows linearity along the whole variability range and R^2 (Pearson) above 0.85; therefore, missing values of the total variable were estimated by the linear regression with the corresponding ion species, and vice versa.

This approach was also used for missing data of S or SO_4^-, by reciprocal stoichiometric conversion. In the case of Mg and Mg^{2+} the regression parameters were not satisfying. In this case, and for all other chemical species included in the dataset, missing values were replaced by season averages calculated over available data, excluding outliers.

2.3. Data analysis

2.3.1. Latent clustering

Cases included in the IAS PM_{10} dataset form clusters of non-independent - nested or hierarchical – observations that, in principle, are not traceable to season or anthropogenic impact differences.

This kind of data structure is commonly described as a problem of linear mixed effects (Harrison et al., 2018). Latent clustering can be due to the grouping influence by environmental factors others than those expected (e.g. emitting sources), i.e. the geographic location, the seasonal and meteorological evolution, the annual variability, the local and regional land-use, the experimental protocols followed to produce the data, etc., and it has been previously observed in datasets of aerosol measurements (Mikkonen et al., 2011; Li et al., 2017; Harrison et al., 2018). However, in this work the latent clustering is documented for the first time, to the authors' knowledge, related to aerosol chemical speciation data. The investigation of latent clusters requires employing mathematical treatments that specifically address the nested structures of the dataset (Sun et al., 2004; Li et al., 2010), but currently none of the existing methods has been tested on aerosol chemical data. Therefore, a novel methodology was developed (Pietrodangelo et al., Personal communication) to identify latent clusters in the IAS PM_{10} dataset, assess their statistical and physical soundness, and disaggregate significant clusters from each other to the goal of investigating for the hidden presence of unexpected grouping factors (environmental predictors) among cases and chemical variables.

While addressing the hierarchical structure of chemical speciation data is not within the scopes of this work, the improved information obtained by investigating some basic cases of latent clusters in the IAS PM_{10} dataset is discussed in Section 3.4.

2.3.2. Positive matrix factorization

Positive matrix factorization (PMF) (Paatero and Tapper, 1994) is a well-known receptor model which exploits the principle of mass conservation (see Section S4 for details) and relies on the statistical multivariate analysis approach. The input data consist in chemically characterized PM datasets containing key species tracing specific sources (typically primary aerosol species not subjected to chemical transformations in the atmosphere) and the output result is the attribution of PM mass to the different sources identified by the model. It is noteworthy that the main disadvantage of such approach is related to

Table 1

Brief description of the cities, sites, and years/seasons which cases of the IAS PM$_{10}$ dataset refer to. Abbreviations: *sme*: small and medium enterprises; *S*: summer; *W*: winter. (*) Population density refers to years of sample collection by city. For multi-year periods, population density is reported for the first and last year of the period, respectively (Istat, 2023).

City	Geography	Landscape and urban context	Site name	Coordinates	Year(s)/seasons	Population density (*) (inhab/km^2)	Literature
Torino	North-west/Italian Alps, Northern Po Valley	Flat/hilly, pre-alpine, business city, industries in the outskirts (foundries, automotive)	Consolata	45° 4′31.79″N, 7°40′42.35″E	2007, 2011/all seasons	128–130	Padoan et al., 2016; Diana et al., 2023
			Grassi	45° 6′29.37″N, 7°40′39.39″E			
Varese	North-west/Alpine foothills, lakes	Hilly/pre-alpine, industries in the outskirts (food, automotive)	Vidoletti	45°50′15.07″N, 8°48′17.35″E	2012/S, W	1464	Air quality network data (not published)
Monza	North-west/Northern Po Valley, rivers	Flat/country, industries in the outskirts (sme)	Monza Parco	45°36′8.58″N, 9°16′31.26″E	2007–2009 (average)/S, W	368 (year: 2008)	Air quality network data (not published)
Milano	North-west/Northern Po Valley	Flat, business city, tertiary sector, industries in the outskirts (pharmaceutical, manufacturing)	Città Studi, University campus	45°28′35.49″N, 9°13′50.95″E	2006/S, W	6948–7045	Bernardoni et al., 2011
			Città Studi, air quality station Pascal	45°28′43.66″N, 9°13′52.13″E	2012/S, W		Air quality network data (Amato et al., 2016; Daellenbach et al., 2023)
Venezia	North-east/Gulf of Venice, Adriatic coastline	Lagoon, small island and canals, commercial and touristic harbours	Punta Sabbioni	45°25′36.13″N, 12°26′1.26″E	2007/all seasons	636	Masiol et al., 2010; Masiol et al., 2012
Ferrara	North-east/Eastern Po Valley, Adriatic coastline	Flat/country, agriculture, industrial area in the outskirts (power plant, waste incinerator)	Porotto-Cassana	44°51′10.04″N, 11°33′11.41″E	2007, 2011, 2014, 2015/S, W	326–330	Perrino et al., 2014
Bologna	North-east/Southeastern Po Valley, Northern Apennines	Flat/country, intensive agriculture, industries in the outskirts (waste incinerator)	Università	44°29′46.60″N, 11°21′14.72″E	2006/S, W	2608	Tositti et al., 2014
Genova	North-west/Gulf of Genoa, Ligurian coastline, Ligurian Apennines	Hilly/coast, commercial harbour, business city, industrial area in the outskirts	Corso Firenze	44°25′10.65″N, 8°55′38.1″E	2009, 2010, 2015/all seasons	2490–2433	Cuccia et al., 2010; Bove et al., 2018
Rimini	North-east/Adriatic coastline, Southern Po Valley	Flat/seaside, touristic harbour, tourism business	Stadio	44° 3′13.38″N, 12°34′34.88″E	2009, S	1014	Air quality network data (not published)
Riccione	North-east/Adriatic coastline, Southern Po Valley	Flat/seaside, touristic harbour, tourism business	Parco Agolanti	43°59′13.09″N, 12°39′25.19″E	From 2006 to 2011/all seasons (not all years)	1973–2016	Vassura et al., 2014
Pistoia	Central/Florence plain, Chianti hills	Flat/country, plant nursery business, industries in the outskirts (waste incinerator)	Montale	43°54′55.06″N, 11° 0′20.78″E	2014/all seasons	381	Barrera et al., 2015
Sesto Fiorentino	Central/Florence plain, rivers, Morello mountain	Flat/country, agriculture, manufacturing industry	Villa San Lorenzo	43°49′40.30″N, 11°11′39.30″E	2006/all seasons	955	Traversi et al., 2014
Firenze	Central/Florence plain, rivers, Central Apennines	Flat, business city, industrial area in the outskirts (engineering, chemical, pharmaceutical, manufacturing)	Bassi	43°47′8.33″N, 11°17′13.19″E	2006, 2013/all seasons	3484–3632	Nava et al., 2020
Perugia	Central/hills, Central Apennines	Hilly/country, agriculture, tertiary sector, industries in the outskirts (manufacturing, food)	Parco Cortonese	43° 6′23.05″N, 12°21′48.70″E	2013/all seasons	368	Crocchianti et al., 2021
Terni	Central/Nera river basin, Central Apennines	Hilly, large industrial area in the outskirts (AST steel plant, energy production)	Carrara	42°33′37.97″N, 12°39′1.66″E	2016/all seasons	523	Moroni et al., 2012
Civitavecchia	Central/Tirrenian coastline	Flat/coast, commercial and touristic harbour, large industrial area in the outskirts (energy production plants)	Borgo Aurelia	42° 8′5.52″N, 11°47′10.36″E	From 2008 to 2011/S, W (not all years)	702–705	Air quality network data (not published)
			Parco Antonelli	42° 5′28.63″N, 11°48′6.71″E			
Montelibretti	Central/hills, Central Apennines	Hilly/country, agriculture	Montelibretti	42° 6′20.22″N, 12°38′24.34″E	From 2005 to 2010/all seasons	110–113	Perrino et al., 2002; Yttri et al., 2019
Roma	Central/Tevere valley, hills, Tirrennian coastline	Hilly, business city, tertiary sector, industries in the outskirts (engineering, pharmaceutical, food)	Villa Ada	41°56′2.75″N, 12°30′25.27″E	From 2005 to 2007/all seasons	1994–2009	Perrino et al., 2002
Bari	South/plain, Adriatic coastline	Coast, commercial and touristic harbour, business city,	Pane e pomodoro beach	N 41° 7′ 4.446″, E 16° 53′ 32.599″	2007/S, W	2722	Amodio et al., 2010; Ielpo et al., 2011

Table 1 (*continued*)

City	Geography	Landscape and urban context	Site name	Coordinates	Year(s)/seasons	Population density (*) (inhab/km^2)	Literature
		tertiary sector, industries in the outskirts	San Nicola sport stadium Casamassima	N 41° 5′ 5.019″, E 16° 50′ 24.305″ N 40° 57′ 25.672″, E 16° 55′ 13.396″			
Napoli	South/Gulf of Naples, hills, Tirrenian coastline	Hilly/coast, commercial and touristic harbour, business city, tertiary sector, industries in the outskirts (manufacturing)	San Marcellino	40°50′50.80″N, 14°15′29.14″E	2015/S, W	8216	Chianese et al., 2019
Lecce	South/Salentine plain, Adriatic coastline	Flat/country, tourism business, agriculture, sme	University Campus Codacci- Pisanelli Olivetani Beni Culturali	40°20′0.63″N, 18° 7′17.91″E 40°21′22.12″N, 18°10′1.66″E 40°21′40.95″N,18° 9′55.90″E 40°21′5.93″N, 18° 9′45.14″E	2007, 2012/S, W	373–394	Contini et al., 2010 Air quality network data (not published)

secondary aerosol species (e.g., sulphate, nitrate, ammonium) which cannot be traced back to the original sources of the gaseous precursors (e.g. SO_2, NO_x, and NH_3 for sulphate, nitrate, and ammonium, respectively); as a consequence, for those species receptor models apportion the PM mass to the chemical components and not to the emission sources.

In this work, the PMF analysis has been carried out on the original dataset of PM_{10} mass and chemical species mean values, with the goals of 1) describing the average chemical profile of main source contributions affecting the urban PM_{10} composition at representativeness level of the Italian territory; 2) quantitatively estimating the influence of different urban textures on the same profiles.

The U.S. EPA-PMF v5.0 software (Norris et al., 2014) was used in this work; it is accomplished by the Multilinear Engine (ME-2) platform (Paatero, 1999).

Season average values for PM_{10} mass and chemical species provided by participants were used as input data in the PMF analysis. As already mentioned, only variables with a threshold of 60 % for the minimum data coverage were considered, and missing data were estimated as described in Section 2.2 with an associated uncertainty set at four times the calculated value. Cr and As were excluded from the analysis: the first due to the high amount of missing data (around 40 %), the latter since it gave rise to a noisy unique factor during the first runs of the model. In the end, 110 samples and 21 variables (PM_{10} mass, Cl^-, NO_3^-, SO_4^{--}, Na^+, NH_4^+, K^+, Mg^{++}, OC, EC, Al, Si, Ca, Fe, Mn, Ni, Pb, Cu, Ti, V, and Zn) were used as input in the PMF model. PM_{10} mass was introduced as a total variable with an uncertainty set at four times its value (Kim et al., 2003). The final choice – optimized iteratively during the analysis - for uncertainty associated to each variable was: 20 % for Cl^-, NO_3^-, SO_4^{--}, Na^+, NH_4^+, K^+, Mg^{++}, OC; 15 % for EC; 10 % for Al, Si, Fe, Mn, Cu, Ti; 40 % for Ca, Ni, Pb, V, Zn (these variables were downweighted starting from the 10 % initial uncertainty). Extra modeling uncertainty was set to 10 %. The number of model runs was 30. Bootstrap analysis (BS) and displacement of factor elements (DISP) were also performed to check the robustness of the solution retrieved by PMF (Norris et al., 2014; Paatero et al., 2014).

3. Results and discussion

3.1. Physical soundness of the PM_{10} dataset

In Fig. 2 the apportionment of PM_{10} mass to major contributions (mineral dust, sea spray, secondary inorganic aerosol, organic matter, and fossil fuel combustion) calculated by empirical mass closure is matched against average PM_{10} values from the dataset. When the mass closure is calculated by the originally submitted data (Fig. 2a), for about 70 % of total cases the sum of mass contributions falls within the PM_{10}

standard deviation, indicating that the average chemical composition is overall physically consistent with PM_{10}, with underestimation of PM_{10} mass below 30 %. This is also evident by the regression plot reporting the sum of mass contributions against the average PM_{10}, in the same figure. Thus, for these cases, the average chemical composition data allows an almost complete, while being only qualitative, reconstruction of the PM_{10} mass. For the remaining cases the information on chemical composition and on PM_{10} mass are only partially consistent; average composition is indeed underestimated by 30–70 %, but only three cases strongly underestimate the PM_{10}. It is worth noting that cases with larger discrepancies between PM_{10} and chemical composition data are those totally or partially missing (at data submission) of at least two species among ions, EC/OC, and major elements. Nevertheless, data replacement (Section 2.2) allowed us to consider these cases too, for further data analysis. As shown in Fig. 2b, the mass reconstruction calculated by empirical mass closure after replacement of missing data improved significantly, also driving cases with original incomplete chemical information to a sound regression with the PM_{10} mass concentration, as far as the apportionment to major mass contributions is concerned. Indeed, cases formerly showing reconstruction below 30 % of average PM_{10} (Fig. 2a) improved mass closure results, having been thus finally included in one of the two other groups. Ion balance analysis based on the sum of chemical equivalents of anions and cations, calculated after replacement of missing values, shows mean and median anions/cations ratio of 1.2 with 13 % relative standard deviation. This result confirms that missing data replacement was physically coherent with the original chemical speciation of cases, as also indicated by the parameters of regression between anions and cations (Fig. S1).

3.2. Season differences and the influence of geography

The statistical significance of data was assessed either by season and by anthropogenic impact, prior to further evaluation, as reported in Section S3. In general, differences of season average values resulted statistically significant under the two-tailed Welch's *t*-test for fall and winter, while spring and summer groups share the same distribution for most species in the dataset. Statistical discrepancies of spring-summer with respect to fall-winter data cannot be explained by the size of groups, since both spring and fall include 20 cases, while summer and winter include 36 and 34 cases, respectively. It was thus chosen, for the rest of the work, to discuss results combined into two main seasons, warm (spring-summer) and cold (fall-winter). Since species means were mostly provided for a cold and a warm period related to the same site, the number of cases in the two periods is almost equal. From data in Table 2, it is evident that season differences are not significant for all species.
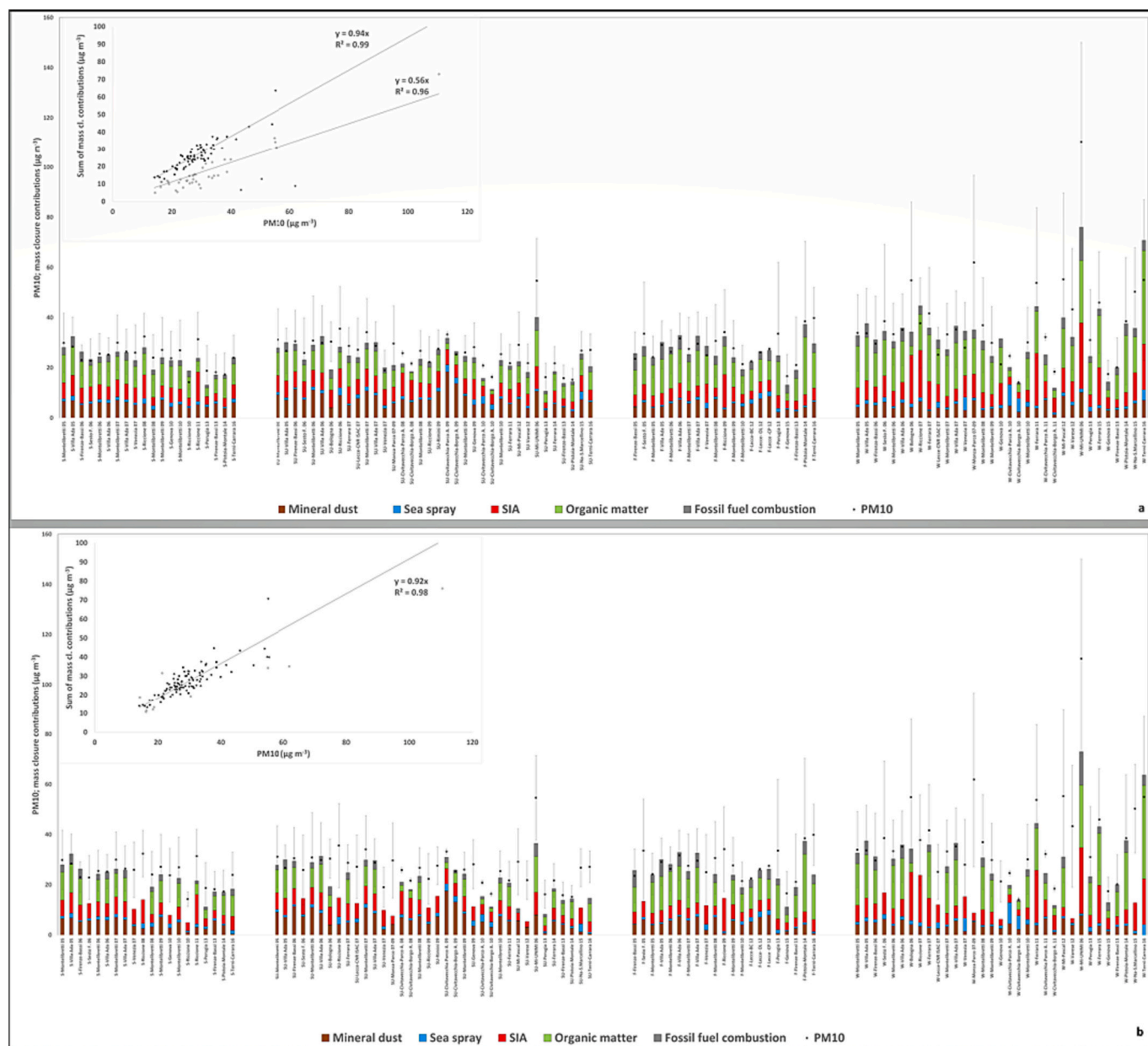
Fig. 2. Apportionment of average PM$_{10}$ to major mass contributions (mineral dust, sea spray, secondary inorganic aerosol (SIA), organic matter and fossil fuel combustion). a: Calculated by using speciation data as originally submitted (including missing values); b: calculated by using speciation data after replacement of missing values. Error bars are given by PM$_{10}$ standard deviation (which here represents the concentration variability not the uncertainties on PM$_{10}$). The regression between the sum of contributions and PM$_{10}$ is also shown, separately for cases for which mass closure reconstruction is above 70 %, within 30–70 % and below 30 % of average PM$_{10}$ (black, light grey and dark grey dots, respectively). S: spring; SU: summer; F: fall; W: winter.

3.2.1. PM$_{10}$ and mass components

Considering the totality of urban sites and years of this study, the PM$_{10}$ mass concentration in the cold season is about 10 µg m^{-3} higher than in the warm period; the *p*-value (Table 2) indicates that the season difference is significant ($p \ll 0.01$). As previously observed, differences are negligible between spring and summer while those between autumn and winter cases are appreciable. However, a sounder differentiation is obtained by combining season with geographical features, i.e., by assigning cases to an 'inland' or 'coast' category based on the distance from coastline, as it is reported in Fig. 3. Since coastlines represent about 80 % of the total perimeter of Italy, the proximity to coast was chosen as the discriminating criterion of geography to be considered. By doing so, it appears evident that only the group of inland cities in the cold season show clearly higher PM$_{10}$ mean values than the other groups,

irrespective of city size.

Furthermore, applying the same combination of criteria to PM$_{10}$ contributions calculated by mass closure, inland cities in the cold season show higher organic matter levels than coastal cities, as it is shown in the inner plot of Fig. 3, although both inland and coastal winter values of this contribution are higher than in the warm season, as expected. This could be likely due to the different strength of biomass burning in the coastal and in the inland areas, being more diffused in the latter, either for domestic heating or farming activities. Concerning other PM$_{10}$ mass components, results obtained by combining season and proximity to coastline do not improve the resolution of differences between inland and coastal urban sites; fossil fuel combustion, mineral dust, sea spray, and SIA show the expected seasonal behaviour as yet previously argued.

Table 2

Season average (standard deviation), warm-cold season difference (standard deviation) and results of the two-tailed Welch's *t*-test of all species of the PM_{10} dataset. Lower *p*-values are associated with a small chance of rejecting the correct null hypothesis of significant season differences. Concentration values are in µg m^{-3} for major species and in ng m^{-3} for minor and trace elements (from As to Zn, as listed in the table).

Species	Warm season aver. (sd)	Cold season aver. (sd)	Test t statistic	P-value	Season difference (sd)
PM10	26 (6.4)	34 (15)	−3.7	4.4E−04	−8.1 (2.2)
Cl^-	0.39 (0.33)	0.61 (0.71)	−2.1	4.3E−02	−0.22 (0.11)
NO_3^-	1.6 (0.98)	3.7 (3.3)	−4.4	3.8E−05	−2.1 (0.46)
$ss\_SO_4^-$	0.16 (0.073)	0.15 (0.13)	0.16	8.8E−01	0.0032 (0.021)
$nss\_SO_4^-$	3.4 (1.1)	2.5 (1.1)	4.4	2.2E−05	0.95 (0.22)
Na^+	0.62 (0.29)	0.61 (0.53)	0.16	8.8E−01	0.013 (0.082)
NH_4^+	0.96 (0.38)	1.2 (1.1)	−1.8	7.0E−02	−0.28 (0.16)
K^+	0.21 (0.10)	0.34 (0.17)	−4.8	5.6E−06	−0.13 (0.027)
Mg^{2+}	0.10 (0.038)	0.095 (0.074)	0.45	6.6E−01	0.051 (0.011)
OC	5.2 (1.9)	9.4 (4.0)	−6.8	2.1E−09	−4.1 (0.61)
EC	1.0 (0.42)	1.8 (0.90)	−5.7	2.6E−07	−0.76 (0.14)
Al	0.30 (0.14)	0.19 (0.10)	4.8	4.9E−06	0.11 (0.024)
Si	0.97 (0.36)	0.61 (0.28)	5.9	5.9E−08	0.36 (0.063)
Ca	1.3 (0.59)	0.95 (0.47)	3.1	2.3E−03	0.32 (0.10)
Fe	0.43 (0.25)	0.47 (0.37)	−0.67	5.0E−01	−0.041 (0.060)
As	0.93 (0.58)	1.4 (0.91)	−3.0	3.8E−03	−0.43 (0.15)
Cr	4.8 (3.7)	4.8 (3.2)	0.011	9.9E−01	0.0072 (0.66)
Mn	11 (6.3)	10 (6.7)	0.74	4.6E−01	0.92 (1.3)
Ni	5.2 (4.5)	5.1 (5.1)	0.14	8.9E−01	0.13 (0.91)
Pb	6.4 (5.5)	12 (12)	−2.9	4.8E−03	−5.2 (1.8)
Cu	20 (9.6)	26 (19)	−2.4	1.9E−02	−6.8 (2.8)
Ti	25 (14)	16 (12)	3.4	1.1E−03	8.4 (2.5)
V	5.9 (5.3)	2.9 (1.5)	4.1	1.3E−04	3.0 (0.74)
Zn	27 (18)	42 (36)	−2.7	9.2E−03	−14 (5.4)

3.2.2. Trace elements

From Table 2, season differences are significant for Cu, Pb, Ti, V and Zn. To assess if these differences are influenced by the geography of cities, the highest values of these species (each individually ordered by decreasing value) at the 50th percentile were evaluated with respect to percent abundance of the season-versus-proximity to coastline combination, which was previously explored in Section 3.2.1; results are reported in Table S1. The 50th percentile value corresponds to an overall flattening of the decreasing curve of elemental concentrations, with the only exception of Ti. Concerning Cu, Pb and Zn, in the cold period their mean concentration is far higher in the inland cities; nevertheless, in the same season Rome also shows high values of Cu and Zn, despite its closeness to coastline. Most of the cities in the 'cold-in' group and the city of Rome are both located in flat or hilly areas included in valleys (see Table 1 for details), that is, a topographical context that aids the triggering of atmospheric stability and thermal inversions episodes in the cold season, favouring the accumulation of pollutants. For Ti and V, as source tracers of desert dust and shipping emissions, respectively, the differences among the four groups (cold -in/co and warm -in/co) seem to be only modulated by the season, aside from the distance from the coastline. Most of the highest mean values occur in the warm period, coherently with the more frequent events registered in this season for medium-long range transport of desert dust to the Italian territory and stronger emissions from shipping activities, either local (high V values are indeed associated to cities with commercial ports, in Table S1) or transported.

3.3. Variability of the urban PM_{10} chemical composition with city size and anthropogenic impact

3.3.1. City size

Population density of cities was used as a proxy of the city size and it was calculated for the respective years which cases refer to (Istat, 2023). Cases were grouped into three clusters, under the criteria of the OECD categorization by size of urban agglomerations (OECD, 2021). This produced clusters of similar numerosity (ranging 34–40 cases) within
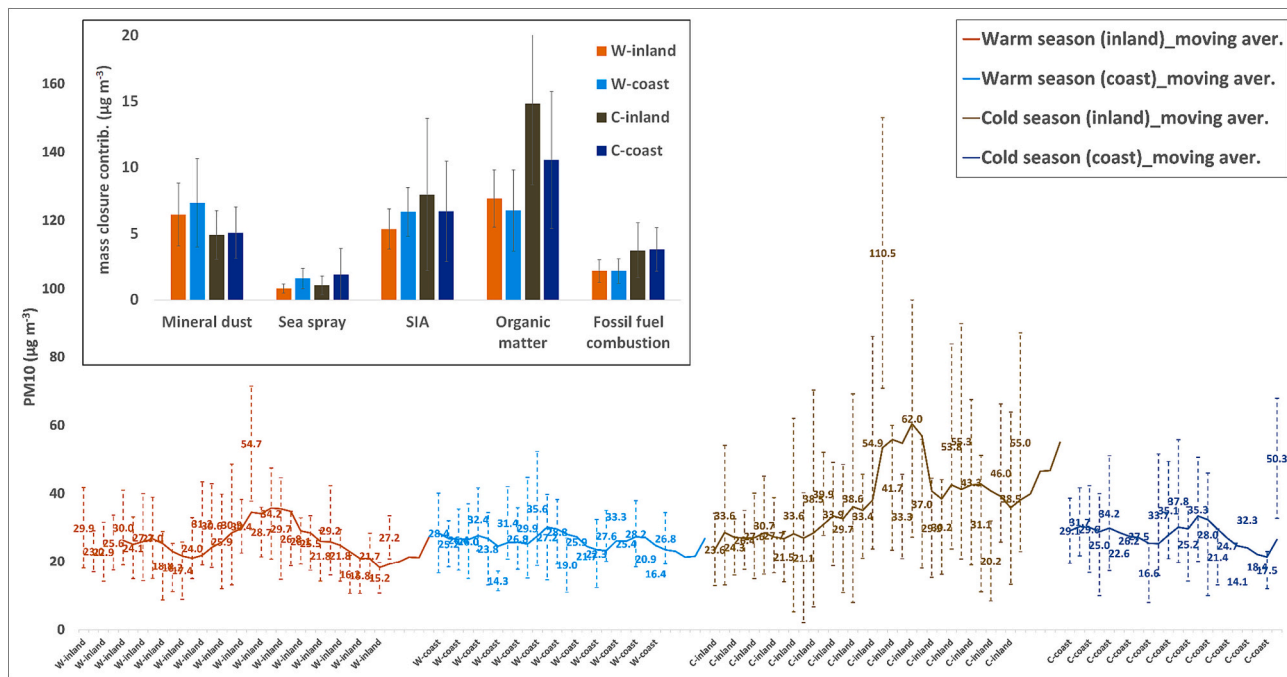

Fig. 3. PM_{10} mean values reported by combining season (warm (W)/cold (C)) and proximity to coastline (inland/coast) site information. Error bars are standard deviation submitted with mean values. Lines are moving averages by a fixed subset of 5, for each group. The highest values in the W-inland, C-inland and C-coast groups refer to Milano in 2006 (54.7 and 111 µg m^{-3}) and Napoli in 2015 (50.3 µg m^{-3}), respectively. In the inner plot, PM_{10} contributions calculated by mass closure are also reported by combined criteria of season and proximity to coastline.

the following ranges of population density (number of individuals per square km): ≥2000 (*large*; Torino, Napoli, Milano, Firenze, Bologna, Genova, Roma, Riccione, Bari), 400–2000 (*medium*; Varese, Rimini, Sesto Fiorentino, Civitavecchia, Venezia, Terni, Lecce, Pistoia) and <400 (*small*; Monza, Ferrara, Montelibretti, Perugia). The relative mass of each species in the PM_{10} was considered in this part of the study, to highlight the possible relationship with differences in the chemical enrichment of the PM_{10} mass. Differences among groups resulted poorly significant under the two-tailed Welch's *t*-test for most species. However, for EC, Fe, and Cu the test evidenced significant differences at 95 % confidence level between population density groups, as shown in Fig. 4, where the PM_{10} mass concentration clustered by the same groups is also reported. The null hypothesis of similarity between groups is accepted by the Welch's *t*-test in the case of PM_{10}, suggesting that the population density does not critically influence the PM_{10} mass concentration, while it is rejected for EC, Cu, and Fe. The chemical enrichment of PM_{10} mass in these species, which are well-known source tracers of the vehicular traffic (Viana et al., 2008), is thus significantly affected by differences of population density. In particular, largely populated cities have significantly higher EC and Cu levels than cities with medium and small density (for EC: 1.8 and 1.2–1.4 µg m^{-3} on average, respectively; for Cu: 1 and 0.6–0.7 ng m^{-3} on average, respectively), while Fe is more abundant in both large and medium density cities with respect to small ones (on average 18–19 and 8 ng m^{-3}, respectively). It is plausible that similar differences would be observed for other specific traffic-related chemical tracers, which are however not available for this dataset.

The null hypothesis of similarity is also rejected when the Ni and V mass concentration in PM_{10} is compared among the population density groups. Cities in the group 400–2000 show significantly higher Ni and V concentrations than other groups. Cities in the dataset having medium density population are indeed also those more impacted by large harbours (Venezia, Civitavecchia) or by industrial sites in the proximity of the urban area (Terni). These cities are thus more affected by Ni than highly populated cities, as reported in Fig. S2, except for Genova (in the >2000 density group), where high Ni and V concentration in the PM_{10} is also observed, due to the strong influence of port activities.

3.3.2. Anthropogenic impact

To evaluate the anthropogenic impact, the business demography was used as parameter, which describes the active population of enterprises within a region and a given period, by means of indicators that include activities relating to industry, construction, distributive trades and services, thus reflecting the influence of main working sectors on the territory (Eurostat, 2022b). In this part of the study, the cases were a-priori assigned to categories based on the business demography statistics applied to Italian provinces for the year 2016 (Istat, 2020), to investigate the link between working activities and urban PM_{10} composition. Categories were defined depending on the number of newborn enterprises in 2016, namely: >500 (Torino, Milano and Roma), 50–500 (Bologna, Firenze, Varese, Pistoia and Monza: 51–100 or 101–500 new enterprises) and <50 (Ferrara, Terni, Lecce, Sesto F., Perugia, and Montelibretti).

A *harbour* category (including Venezia, Genova, Civitavecchia, Napoli, Bari, Rimini and Riccione), which includes cities with commercial and/or touristic ports, has been also considered separately, to specifically evaluate the impact of port enterprises and activities, given the large number of coastline cities in Italy. Port cities listed above fall in the >500 (Venezia, Civitavecchia, Napoli), 50–500 (Genova, Bari), and <50 (Riccione and Rimini) classes.

Concerning differences of species concentration in the PM_{10} mass, from Fig. S3 it is evident that the dataset response to clustering by business demography is sharper compared to using population density. With respect to the latter, cities in the highest business demography class are more affected by Cu, while all other cities show comparable Cu variability ranges and mean value. All cities with >100 newborn enterprises instead show comparable variability of Fe and EC, coherently with increased traffic fluxes and public transportation frequency due to business-driven rush. As reasonably expected, port cities distinguish from the rest mostly for shipping activities, as indicated by the far larger mean and variability ranges of Ni and V, independently of the port city size and population density. Nevertheless, the influence of in-harbour and maritime procedures seems also to be inferred by this categorization. This is particularly evident in the case of Fe, with mean value of the *harbour* group that is comparable to that of the groups >500 and 50–500, and mass enrichment of Fe in the PM_{10} far above the mean value in about 30 % of cases included in this group.
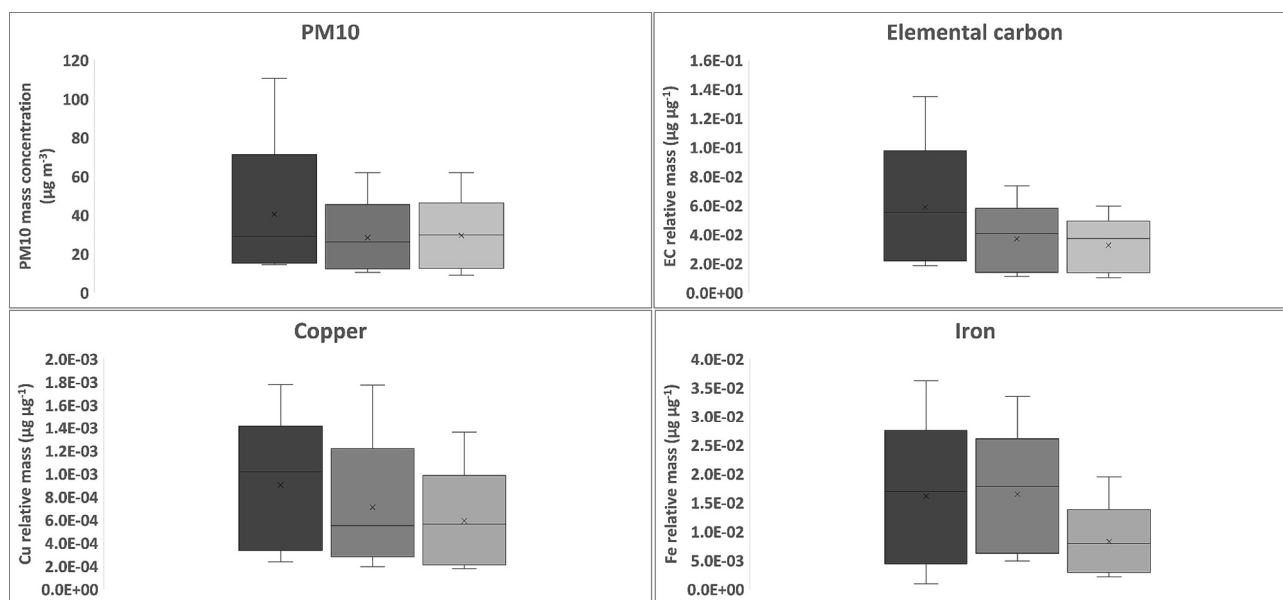

Fig. 4. Box and whiskers plot of the species whose relative mass in the PM_{10} is significantly discriminated among cities with different density of the general population (null hypothesis of similarity rejected by two-tailed Welch's *t*-test, at 95 % confidence level). For each species, cases are grouped by number of individuals per square km; from left to right: ≥2000, 400–2000, <400. The PM_{10} clustered by the same groups is also shown.

3.4. Hidden information in latent clusters: basic examples from the IAS PM_{10} dataset

3.4.1. The Cl^-/Na^+ ratio

The linear regression between Cl and Na ions including all the 110 cases of the dataset is described by a slope of 0.90 (R^2 0.79). However, a large dispersion is observed around the regression line, as shown by the inner plot of Fig. S4, which suggests that subgroups of data points independent of each other might share the same (Na^+, Cl^-) variability domain. The Cl^-/Na^+ ratio shows two sharp inflection points along the decreasing plot (not shown), which identify three groups with averages (% relative standard deviation) of 3.7 (54 %), 1.4 (16 %) and 0.64 (36 %), respectively. When the three groups are plotted separately (main part of Fig. S4), the related linear regressions improve significantly with respect to considering the 110 cases all together. In the figure, the sea salt Cl^-/Na^+ ratio from literature (Seinfeld and Pandis, 2006) has been also plotted starting from the Na^+ values of the 110 cases. Among the three groups, the distribution of the central one (slope 1.4) is close to that of the sea salt, sharing also a similar variability range, both along x and y axes. Concerning the third group, the Cl^-/Na^+ ratio is around 0.64 (range: 0.20–1.1, including 75 % of total cases): similar values are commonly attributed to a partial chloride depletion due to sea salt ageing, in atmospheric aerosol studies (Bondy et al., 2017). Therefore, the second and third groups can be related to cases that were differently affected by sea spray, either fresh or aged from transport, respectively. Finally, in cases with the highest Cl^-/Na^+ ratio (indicated as 'DS_fresh/ aged/Cl^- excess' in Fig. S4) an excess of Cl^- is observed, suggesting that likely further sources as steelworks influenced those cases, in addition to, or differently from, the sea spray.

3.4.2. The V/Ni ratio

The curve of decreasing values of the V/Ni ratio, considered over all cases of the dataset, shows an inflection point at 1.1 (Fig. S5a, inner plot). Interestingly, this threshold seems to sharply discriminate between two groups: cases of the warm season and those of the cold season, with few exceptions; in addition, most cases of port cities also show V/Ni ratio far above 1.1. The linear regression between V and Ni, calculated separately for these three groups, shows that cases with V/Ni ≤ 1.1 distribute along the regression line with much lower slope than the other two groups. The median ($\pm$ standard deviation) of V and Ni concentration for the three groups are: 2.4 ± 1.4 and 3.3 ± 1.7 (V/Ni ≤ 1.1), 5.0 ± 2.0 and 3.3 ± 1.2 (V/Ni >1.1), 7.0 ± 9.7 and 5.6 ± 5.5 (port cities), respectively. It is evident, also looking at Fig. S5a, that the large difference observed among slopes is mainly due to the large increment of V in the V/Ni >1.1 group with respect to cases where the same ratio assumes values below unity. Since the V/Ni ratio is a source-selective indicator of crude oil combustion, particularly relating to the emission of exhausts from shipping (Pey et al., 2013; Corbin et al., 2018; Zhao et al., 2021), all cases of the dataset were investigated with respect to their distance from the reference source profiles of shipping, available from the database SPECIEUROPE (Pernigotti et al., 2016). To this aim a scatter plot was used, which is shown in Fig. S5b; other source profiles of the repository, namely vehicle exhaust emissions and wood burning, were also considered, to improve the interpretation of cases in the scatter plot with respect to other possible influencing sources. In Fig. S5b, the cases of port cities distribute close to reference profiles no. 210, 211, 212 and 287, which relate to exhausts emission from ship auxiliary engines (at three different loads) and to the presence of harbour, respectively; the other shipping profiles, connected to exhaust emissions from the main engine (again, at different loads), are instead distributed far from the above-described cluster.

The use of auxiliary engines in marine vessels is expected during harbour activities and during the stay of the vessel at the dock, to keep on-board power sources on. This supports the hypothesis that the V/Ni values observed for port cities, particularly in the warm season, are due to port activities more than to the medium-long range transport from

open sea of exhaust plumes from vessels sailing. Similar remarks can be applied to the other cases with V/Ni >1.1, which share quite equal linear regression of port cities (Fig. S5a), likely reflecting the influence of the latter on other cities, especially during the warm season. It has to be considered that the distance of very inland cities of Central and South Italy from Adriatic or Tyrrhenian Sea coasts ranges at most 50–100 km, therefore a short- or medium-range transport of air masses from local ports to other cities is probably more frequent than the transport from open sea. Concerning cases with V/Ni ≤ 1.1, in the scatter plot they are chiefly distributed close to vehicle exhaust reference profiles, suggesting a likely increased influence of local traffic emissions, in the cold season, with respect to the transport of polluted plumes from harbours.

3.4.3. Other relevant ratios: OC/EC and Fe/Al

In the IAS PM_{10} dataset, the OC/EC ratio ranges $2 \div 12$, and clear relationships are observed between the variability segments, within the overall interval, and the city type (size, geography). In Fig. S6 the 110 cases of the dataset are reported by decreasing value of OC/EC for the different city sizes (as defined in Section 3.3.1) and dominant geography (Inland, Coastal). It is evident that higher values of the ratio are those of small- and medium-size inland cities, while lower values pertain to large and medium cities, among which most coastal ones, irrespective of the season (not shown). This trend agrees with findings reported by Pio et al. (2011), relating to many European sites differently affected by the anthropogenic burden. In that work, it is shown how the $(OC/EC)_{min}$ ratio decreases from remote to industrial sites because of the increasing EC levels due to the stronger impact of anthropogenic sources. The urban sites included in the IAS PM_{10} dataset confirm these findings. The relative mass of EC in the PM_{10} is plotted in Fig. S6 correspondingly to the OC/EC. It is evident that decreasing OC/EC values are driven by the increasing EC mass concentration in the medium and large cities. This also provides an explanation for the minor relevance of seasonality, since the main factors determining the decreasing trend are the larger city size and the proximity to the sea, both increasing the strength of anthropogenic activities and, consequently, the EC concentration in the PM_{10} mass. Concerning sources of crustal materials, the Fe/Al ratio was considered, since it seems to be more responsive to the influence of anthropogenic activities, with respect to other ratios. Recently, Boraiy et al. (2023) have reported values of Fe/Al above the $0.5 \div 2$ range, which is commonly observed in the natural crustal dust of either African and European origin (Pietrodangelo et al., 2013), at a site strongly impacted by large population density and neighbouring industries. In this work, a similar behaviour is observed for this ratio. The inflection point at Fe/Al values around 2 (inner part of Fig. S7) clearly separates cases in two groups, as it is shown in the main part of Fig. S7. In particular, the cluster with Fe/Al > 2 mainly refers to large and medium cities (90 % of the cities in this group), thus evidencing the influence of the anthropic burden by an evident enrichment in Fe with respect to values expected for mineral dust.

3.5. Positive matrix factorization results

The most reliable and robust PMF solution is the seven-factor constrained analysis. These factors were tentatively labelled according to their characteristic tracers (Viana et al., 2008) as *Marine, Dust1, Dust2, Nitrate, Sulfate and Heavy Oil Combustion, Biomass Burning*, and *Urban* aerosol. This assignment takes into account the major drawback of receptor models, which can apportion the contributions of secondary components to PM mass as such, without any chance to relate them to the source of gaseous precursors.

In this PMF analysis, two constraints were applied to the *Nitrate* factor profile, pulling down maximally Pb and Zn which are typical of primary anthropogenic emissions more related to the *Urban* factor. The maximum variation allowed in Q for the applied constraint was 10 %, with a final dQ variation of 4 % compared to base solution.

For the best solution, chemical profiles (in $\mu g\ m^{-3}$) and the share of

components in terms of percent contributions are shown in Fig. S8 and Fig. 5. The average PM_{10} mass apportionment (in %) at each site averaged over all results retrieved for the cold and warm periods is reported in Fig. 6.

The robustness of the final solution was evaluated by bootstrap analysis (100 runs) and all factors resulted very well mapped with unmapped cases limited to 1 % (for *Nitrate* source profile). Moreover, the dQ-controlled perturbation or displacement of factor profile (DISP) analysis was performed to assess the rotational ambiguity on the selected solution; overall, the main tracers in the profiles showed quite narrow DISP intervals. A summary of the solution uncertainty assessment using BS and DISP from EPA-PMF is reported in the Supplementary Material (Fig. S9).

The *Marine* factor chemical profile is characterized by the typical sea salt tracers, i.e., Na^+, Cl^-, and Mg^{2+} as reported in Fig. S6. It is noteworthy that highest share in terms of PM_{10} mass (i.e. higher than 10 % see Fig. 6) is typically found at coastal sites and only in few cases at inland sites easily impacted by sea salt transport events due to their geographical position (e.g. Lecce); only in a couple of cases (i.e. Varese and Perugia) the apportioned mass for this factor was about 10–15 % although the sites are scarcely impacted by marine air masses.

Al and Si - typical tracers of mineral particles – show quite comparable shares in both *Dust1* and *Dust2* factors but the percent contribution of other species significantly differ (see Fig. S6); this is the case of Ca which is a dominant species in the *Dust2* factor (ca. 60 % in *Dust2* vs. 0.7 % in *Dust1*). Not negligible percentages of Fe, Mn, and Ti (elements also present in the Earth's crust) as well as V and Ni (typical tracers for heavy oil combustion) characterize the *Dust1* factor. The difference in composition suggests that likely *Dust1* is more representative of mineral dust transported from long distances which overpassed areas with Ni and V emissions from heavy oil combustions (either from shipping or industrial plants). Opposite, *Dust2* might be more representative for local dust resuspension with a contribution from road dust and/or construction works as suggested by Ca enrichment (see e.g., Amato et al., 2009; Pio et al., 2022). Mass contributions of *Dust1* and *Dust2* (summed up together) vary in the range 12–64 % and 0–38 % in the warm and cold periods, respectively, among sites.

As expected, a relevant mass contribution (>15 %) of the *Nitrate* factor is detected during the cold period and the highest values (i.e. >30 %) are found at sites located in the Po valley (see e.g., Vecchi et al., 2018; Scotto et al., 2021), a well-known hot spot for aerosol secondary components; the only exception is Napoli where 49 % of the PM_{10} mass in the cold period is apportioned by this factor. The other factor expected to dominate mass contributions during the cold periods is *Biomass burning* as being characterized by high contributions of OC, EC, and K^+ in the source profile (Cachier et al., 1991; Belis et al., 2011; Pio et al., 2022; and therein cited references) and by high species percent contributions. In the large majority of the sites where biomass burning accounts for more than e.g. 20 % of the PM_{10} mass it occurs during the cold period but is also interesting to note not negligible contributions are

also detected during the warm period; more generally, 73 % of the sites show contributions higher than 10 % to PM_{10} mass. These results can be explained considering that – in addition to biomass burning due to domestic heating in cold periods – emissions from neighbouring agricultural (e.g. it is usual to burn crop straw is in fields after harvest) and cooking (e.g. pizzerias with wood oven, which are widespread in Italy) activities are very likely (Scotto et al., 2021).

The factor with the chemical profile dominated by SO_4^{2--}, NH_4^+, V, and Ni was named *Sulfate and Heavy Oil combustion*. V and Ni are typical tracers for heavy oil combustion which can be related to industrial and shipping emissions (Viana et al., 2008; Bove et al., 2014; Contini and Merico, 2021). Sulphate is generally associated with regional pollution. This factor contributes up to 45–47 % of the PM_{10} during the warm periods in Bologna and Venezia.

The factor labelled as *Urban*, is characterized by significant heavy metals contributions (e.g. Pb, Cu, Zn, Fe) but also EC and OC (see e.g., D'Alessandro et al., 2003; Viana et al., 2008; Amato et al., 2016). These are all tracers of anthropogenic emissions like traffic and industrial emissions and half of the sites show PM_{10} mass contributions higher than 20 %.

The soundness of the PMF profiles has been evaluated by comparison against the source profiles of the database SPECIEUROPE, assumed as reference. To this aim, the standardised identity distance (SID) was employed, as described by Belis et al. (2015a), which is a similarity test assessing the comparability between source profiles that are expected to refer to the same source category. The SID is calculated based on the ratio - over all species j of two profiles a and b - of the identity distance (ID) to the maximum accepted distance (MAD). These quantities are calculated by each species and can be geometrically interpreted, respectively, as the distance of the profile from the identity (one-to-one) line, and the lower and upper threshold distances from the identity line within which the ID is acceptable; SID values above unity indicate that the two profiles are poorly or not comparable. A full presentation and application of this approach is described in Belis et al. (2015a, 2015b). In Figs. S10 and S11 two PMF profiles of this work, namely *Biomass burning* and *Dust2*, are plotted each against different reference profiles of the same source category; the lower and upper acceptability thresholds are also reported for each comparison. Reference profiles of Figs. S10 and S11 were selected by applying the best compromise between the lowest values of SID (relating to the comparison of PMF with reference profiles) and the completeness of reference profiles in terms of available species. It is worth noting that SID values were far below unity in all comparisons, but with large variability between the minimum (8 10^{-3} and 2 10^{-3}) and the maximum (3 10^{-2} and 6 10^{-3}) values for the biomass burning and the dust profiles, respectively; the number of profiles evaluated for each source category was similar, namely 22 for biomass burning and 21 for road dust (plus additional four profiles of brake and tyre wearing). Concerning biomass burning, the PMF profile shows poor comparability with profile #192 (Fig. S10a), while the comparability with profiles # 5, 6, 7, 8 (Fig. S10b, reported as composite
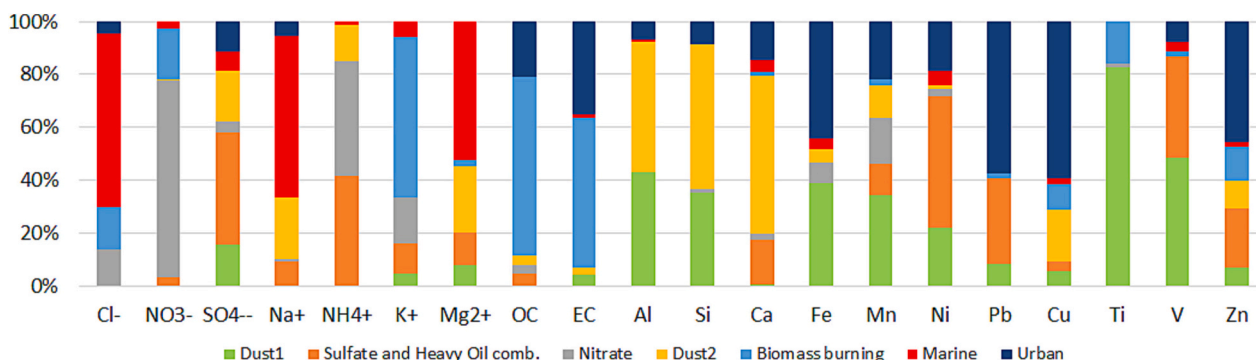

Fig. 5. Sharing of chemical species (percent contributions) in the factor profiles extracted by the best PMF solution.
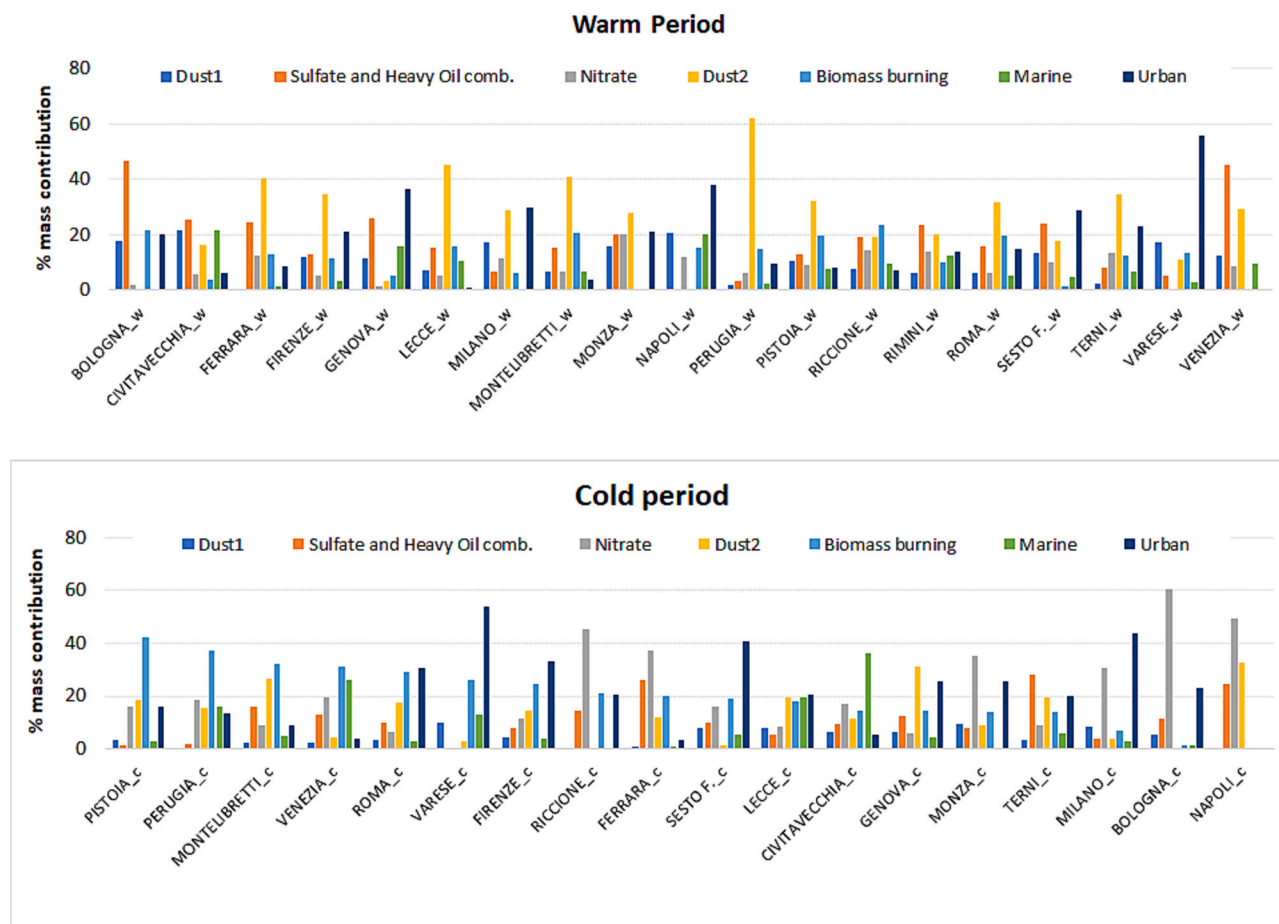
Fig. 6. Mean PM$_{10}$ source contributions (in %) averaged over all results retrieved for the warm (w) and cold (c) periods at each investigated site.

of the four profiles) is fairly good, since all available species are within the acceptability area, with few exceptions (NO$_3^-$, Al, Mn, Ti, and V). This result is coherent with the urban character of the studied sites, whereas open burning is more expected in sites like, e.g., rural areas impacted by agriculture. In the case of the *Dust2* profile of the PMF solution, the lowest SID value is with the profile #52; however, the species available from this profile are far less than those from profile #228. The comparison was thus performed with the latter profile (Fig. S11a), also given the fact that the related SID value is the second lowest of this group. Tracer species of road dust, among those available from the IAS PM$_{10}$ dataset, fall within the acceptability area except for Fe and EC, supporting the affinity of the *Dust2* profile with the road dust source category. Differently, the comparison with the brakes/tyre wearing sub-category (Fig. S11b), following the same criteria as above described, suggests that the *Dust2* profile does not include the influence of wearing processes that affect vehicle mechanical components. Indeed, the lowest SID between the *Dust2* and the brakes/tyre wearing sub-category is anyway far higher than values relating to the road dust category. The reference profiles used for comparison all over this work are cited with the original ID number of SPECIEUROPE.

4. Conclusions

This work proposes a novel methodology to generate a PM chemical speciation dataset with atypical time resolution (e.g., season averages over the years 2005–2016) and wide spatial coverage (here >20 cities over the whole Italian territory) suitable for a receptor model study. Indeed, average values used in this work as input to the PMF model have heterogeneous origin - differing among each other by years, site and duration of measurement campaigns generating the data, number of

punctual data collected, and analytical procedures, this condition being typically unfavourable to a sound PMF modeling. Despite this, the results obtained by the model are reliable, as tests of modeling performance demonstrated (namely: SID for similarity with reference profiles, BS and DISP analysis for profile uncertainty assessment).

An added value of the dataset built in this work and the source chemical profiles obtained by PMF analysis is that they can be further used in large variety of experimental and modeling studies as they provide - for the first time with nation-wide representativeness - a general picture of the linkages inter-connecting Italian cities to the peculiar geographical and topographical features of Italy, and to the chemical variability of urban aerosol with special focus on the PM$_{10}$ fraction. It is worth noting that the dataset also provides - by same territorial and seasonal representativeness above mentioned - season averages of minor and trace elements (As, Cr, Mn, Ni, Pb, Cu, Ti, V, and Zn), which are generally not available from other comparable datasets. Results of tests on the physical consistency and the statistical significance of the chemical speciation data indicate that the IAS PM$_{10}$ dataset has a potential for employment as a reference repository of season averages for the chemical species, relating to the Italian territory. Averages can be extracted from the dataset depending on the target and the city under study, by aggregating chemical data for the geographical area, topographical features, business intensity or population density, combined to season.

The application of the proposed methodology to the IAS PM$_{10}$ dataset shows that among the 21 urban agglomerations included, significant relative differences in the PM$_{10}$ composition refer to two city-geography types: 1) inland cities with high (Torino, Milano, Roma) or medium (Bologna, Firenze, Varese, Monza and Pistoia) anthropogenic impact due to business and to large- or medium-size population density;

2) port cities, especially those with commercial harbours (Venezia, Genova, Civitavecchia and Napoli). Inland cities of Italy are mostly located in flat or hilly areas extending within valleys: this topography aids the occurrence of atmospheric stability and thermal inversion episodes, particularly in the Po plain but also common to many basins of the Apennines and the Alps, with consequent pollutants accumulation (Ferrero et al., 2014) due to the emissions mainly related to biomass burning for domestic heating and traffic. Port cities, on the other side, are interested by frequent wind advection and air mixing that reduce the pollutants accumulation because of the proximity to the coastline. Nevertheless, at port cities the PM_{10} is affected by higher mass contributions of sea spray (in both warm and cold seasons) and, to minor extent, of mineral dust from long-range transport in the warm period. In addition, port cities show – whatever the size - the largest enrichment in V and Ni, mainly due to in-harbour activities, and a significant enrichment in Fe. These findings indicate that this approach is powerful, and it could be further employed with other dataset of atypical chemically speciated data, like those available in the EU Countries, from sampling points of air pollution monitoring networks where the $PM_{2.5}$ chemical speciation is required, under the 2008/50/EC Directive for Air Quality and its ongoing revision. In addition, the chemical profiles obtained could be proposed as a contribution to profiles repositories, like SPE-CIEUROPE, since they refer to a large number of Italian cities and can be thus considered as representative at territorial scale, that is, of the source profiles commonly measured at urban agglomerations of Italy.

CRediT authorship contribution statement

Adriana Pietrodangelo: Conceptualization, Methodology, Investigation, Formal analysis, Writing – original draft, Writing – review & editing. **Maria Chiara Bove:** Conceptualization, Formal analysis, Investigation, Writing – original draft, Writing – review & editing. **Alice Corina Forello:** Conceptualization, Formal analysis, Investigation, Writing – original draft, Writing – review & editing. **Federica Crova:** Formal analysis, Investigation, Writing – original draft, Writing – review & editing. **Alessandro Bigi:** Conceptualization, Methodology, Writing – review & editing. **Erika Brattich:** Conceptualization, Methodology, Writing – review & editing. **Angelo Riccio:** Conceptualization, Methodology, Writing – review & editing. **Silvia Becagli:** Data curation, Writing – review & editing. **Stefano Bertinetti:** Data curation, Writing – review & editing. **Giulia Calzolai:** Data curation, Writing – review & editing. **Silvia Canepari:** Data curation, Writing – review & editing. **David Cappelletti:** Data curation, Writing – review & editing. **Maria Catrambone:** Data curation, Writing – review & editing. **Daniela Cesari:** Data curation, Writing – review & editing. **Cristina Colombi:** Data curation, Writing – review & editing. **Daniele Contini:** Data curation, Writing – review & editing. **Eleonora Cuccia:** Data curation, Writing – review & editing. **Gianluigi De Gennaro:** Data curation, Writing – review & editing. **Alessandra Genga:** Data curation, Writing – review & editing. **Pierina Ielpo:** Data curation, Writing – review & editing. **Franco Lucarelli:** Data curation, Writing – review & editing. **Mery Malandrino:** Data curation, Writing – review & editing. **Mauro Masiol:** Data curation, Writing – review & editing. **Dario Massabò:** Data curation, Writing – review & editing. **Cinzia Perrino:** Data curation, Writing – review & editing. **Paolo Prati:** Data curation, Writing – review & editing. **Tiziana Siciliano:** Data curation, Writing – review & editing. **Laura Tositti:** Data curation, Writing – review & editing. **Elisa Venturini:** Data curation, Writing – review & editing. **Roberta Vecchi:** Conceptualization, Methodology, Investigation, Writing – original draft, Writing – review & editing.

Declaration of competing interest

The authors declare that they have no known competing financial interests or personal relationships that could have appeared to influence the work reported in this paper.

Data availability

Data are available on request. Please contact Adriana Pietrodangelo (pietrodangelo@iia.cnr.it).

Appendix A. Supplementary data

Supplementary data to this article can be found online at https://doi.org/10.1016/j.scitotenv.2023.167891.

References

Amato, F., Pandolfi, M., Viana, M., Querol, X., Alastuey, A., Moreno, T., 2009. Spatial and chemical patterns of PM10 in road dust deposited in urban environment. Atmos. Environ. 43, 1650–1659. https://doi.org/10.1016/j.atmosenv.2008.12.009.

Amato, F., Alastuey, A., Karanasiou, A., Lucarelli, F., Nava, S., Calzolai, G., Severi, M., Becagli, S., Gianelle, V.L., Colombi, C., Alves, C., Custodio, D., Nunes, T., Cerqueira, M., Pio, C., Eleftheriadis, K., Diapouli, E., Reche, C., Minguillon, M.C., Manousakas, M.I., Maggos, T., Vratolis, S., Harrison, R.M., Querol, X., 2016. AIRUSE-LIFE+: a harmonized PM speciation, source apportionment in five~southern European cities. Atmos. Chem. Phys. 16 (5), 3289–3309. https://doi.org/10.5194/acp-16-3289-2016.

Amato-Lourenco, L.F., Lobo, D.J.A., Guimarães, E.T., Lopes Moreira, T.C., Carvalho-Oliveira, R., Saiki, M., Saldiva, P.H.N., Mauad, T., 2017. Biomonitoring of genotoxic effects and elemental accumulation derived from air pollution in community urban gardens. Sci. Total Environ. 575, 1438–1444. https://doi.org/10.1016/j.scitotenv.2016.09.221.

Amodio, M., Andriani, E., Cafagna, I., Caselli, M., Daresta, B.E., de Gennaro, G., Di Gilio, A., Placentino, C.M., Tutino, M., 2010. A statistical investigation about sources of PM in South Italy. Atmos. Res. 98, 207–218.

Arias, P.A., Bellouin, E., Jones, R.G., Krinner, G., Marotzke, J., Naik, V., Palmer, M.D., Plattner, G.-K., J.R., Rojas, M., Sillmann, J., Storelvmo, T., Thorne, P.W., Trewin, B., Rao, K. Achuta, Adhikary, B., Allan, R.P., Armour, K., G.B., Barimalala, R., Berger, S., Canadell, J.G., Cassou, C., Cherchi, A., Collins, W., Collins, W.D., Connors, S.L., Corti, S., F.C., Dentener, F.J., Dereczynski, C., Di Luca, A., Niang, A. Diongue, Doblas-Reyes, F.J., Dosio, A., Douville, H., F.E., Eyring, V., Fischer, E., Forster, P., Fox-Kemper, B., Fuglestvedt, J.S., Fyfe, J.C., Gillett, N.P., Goldfarb, L., I.G., Gutierrez, J.M., Hamdi, R., Hawkins, E., Hewitt, H.T., Hope, P., Islam, A.S., Jones, C., Kaufman, D.S., Kopp, R.E., Y.K., Kossin, J., Krakovska, S., Lee, J.-Y., Li, J., Mauritsen, T., Maycock, T.K., Meinshausen, M., Min, S.-K., P.M.S.M., Ngo-Duc, T., Otto, F., Pinto, I., Pirani, A., Raghavan, K., Ranasinghe, R., Ruane, A.C., Ruiz, L., Sallée, J.-B., B.H.S., Sathyendranath, S., Seneviratne, S.I., Sörensson, A.A., Szopa, S., Takayabu, I., Tréguier, A.-M., van den Hurk, B., R.V., von Schuckmann, K., Zaehle, S., Zhang, X., K.Z., 2021. Technical summary. In: Climate Change 2021: The Physical Science Basis. Contribution of Working Group I to the Sixth Assessment Report of the Intergovernmental Panel on Climate Change. Cambridge University Press, Cambridge, United Kingdom and New York, NY, USA. https://doi.org/10.1017/9781009157896.002. Persistent URL. https://www.dora.lib4ri.ch/wsl/islandora/object/wsl:2839.

ARPA Umbria, 2016. Available at: https://www.arpa.umbria.it/articoli/caratteristiche-morfologiche-e-chimiche-delle-polv.

Barrera, V., Calzolai, G., Chiari, M., Lucarelli, F., Nava, S., Giannoni, M., Becagli, S., Frosini, D., 2015. Study of air pollution in the proximity of a waste incinerator. Nucl. Instrum. Methods Phys. Res. B 363, 112–118. https://doi.org/10.1016/j.nimb.2015.08.015.

Belis, C.A., Cancelinha, J., Duane, M., Forcina, V., Pedroni, V., Passarella, R., Tanet, G., Douglas, K., Piazzalunga, A., Bolzacchini, E., Sangiorgi, G., Perrone, M.-G., Ferrero, L., Fermo, P., Larsen, B.R., 2011. Sources for PM air pollution in the Po Plain, Italy: I. Critical comparison of methods for estimating biomass burning contributions to benzo(a)pyrene. Atmos. Environ. 45 (39), 7266–7275. https://doi.org/10.1016/j.atmosenv.2011.08.061.

Belis, C.A., Pernigotti, D., Karagulian, F., Pirovano, G., Larsen, B.R., Gerboles, M., Hopke, P.K., 2015a. A new methodology to assess the performance and uncertainty

of source apportionment models in intercomparison exercises. Atmos. Environ. 119, 35–44. https://doi.org/10.1016/j.atmosenv.2015.08.002.

Belis, C.A., Karagulian, F., Amato, F., Almeida, M., Artaxo, P., Beddows, D.C.S., Bernardoni, V., Bove, M.C., Carbone, S., Cesari, D., Contini, D., Cuccia, E., Diapouli, E., Eleftheriadis, K., Favez, O., El Haddad, I., Harrison, R.M., Hellebust, S., Hovorka, J., Jang, E., Jorquera, H., Kammermeier, T., Karl, M., Lucarelli, F., Mooibroek, D., Nava, S., Nøjgaard, J.K., Paatero, P., Pandolfi, M., Perrone, M.G., Petit, J.E., Pietrodangelo, A., Pokorná, P., Prati, P., Prevot, A.S.H., Quass, U., Querol, X., Saraga, D., Sciare, J., Sfetsos, A., Valli, G., Vecchi, R., Vestenius, M., Yubero, E., Hopke, P.K., 2015b. A new methodology to assess the performance and uncertainty of source apportionment models II: the results of two European intercomparison exercises. Atmos. Environ. 123 (Part A), 240–250. https://doi.org/10.1016/j.atmosenv.2015.10.068.

Belis, C., Favez, O., Mircea, M., Diapouli, E., Manousakas, M., Vratolis, S., Gilardoni, S., Paglione, M., Decesari, S., Mocnik, G., Mooibroek, D., Salvador, P., Takahama, S., Vecchi, R., Paatero, P., 2019. European Guide on Air Pollution Source Apportionment With Receptor Models, EUR 29816 EN. Publications Office of the European Union, Luxembourg. https://doi.org/10.2760/439106. ISBN 978-92-76-09001-4. (JRC117306).

Bellouin, N., Quaas, J., Gryspeerdt, E., Kinne, S., Stier, P., Watson-Parris, D., Boucher, O., Carslaw, K.S., Christensen, M., Daniau, A.L., Dufresne, J.L., Feingold, G., Fiedler, S., Forster, P., Gettelman, A., Haywood, J.M., Lohmann, U., Malavelle, F., Mauritsen, T., McCoy, D.T., Myhre, G., Mülmenstädt, J., Neubauer, D., Possner, A., Rugenstein, M., Sato, Y., Schulz, M., Schwartz, S.E., Sourdeval, O., Storelvmo, T., Toll, V., Winker, D., Stevens, B., 2020. Bounding global aerosol radiative forcing of climate change. Rev. Geophys. 58 (1) https://doi.org/10.1029/2019RG000660 e2019RG000660.

Bernardoni, V., Vecchi, R., Valli, G., Piazzalunga, A., Fermo, P., 2011. PM10 source apportionment in Milan (Italy) using time-resolved data. Sci. Total Environ. 409, 4788–4795. https://doi.org/10.1016/j.scitotenv.2011.07.048.

Bondy, A.L., Wang, B., Laskin, A., Craig, R.L., Nhliziyo, M.V., Bertman, S.B., Pratt, K.A., Shepson, P.B., Ault, A.P., 2017. Inland sea spray aerosol transport and incomplete chloride depletion: varying degrees of reactive processing observed during SOAS. Environ. Sci. Technol. 51 (17), 9533–9542. https://doi.org/10.1021/acs.est.7b02085.

Boraiy, M., El-Metwally, M., Borbon, A., Chevaillier, S., Laurent, B., Lafon, S., El Sanabary, F.F., Masmoudi, M., Alfaro, S.C., 2023. Elemental ratios as tracers of the sources of mineral dust in north-eastern Sahara. Int. J. Environ. Sci. Technol. https://doi.org/10.1007/s13762-023-05077-3.

Bove, M.C., Brotto, P., Cassola, F., Cuccia, E., Massabò, D., Mazzino, A., Piazzalunga, A., Prati, P., 2014. An integrated PM2.5 source apportionment study: positive matrix factorisation vs. the chemical transport model CAMx. Atmos. Environ. 94, 274–286. https://doi.org/10.1016/j.atmosenv.2014.05.039.

Bove, M.C., Massabò, D., Prati, P., 2018. PMF5.0 vs CMB8.2: an inter-comparison study based on the new European SPECIEUROPE database. Atmos. Res. 201, 181–188.

Cachier, H., Ducret, J., Bremond, M.P., Gaudichet, A., Lacaux, J.P., Yoboue, V., Baudet, J., 1991. Characterisation of biomass burning aerosols in savanna region of the Ivory Coast. In: Levine, J. (Ed.), Global Biomass Burning. MIT Press, Cambridge, Mass, pp. 174–180.

Carbone, C., Decesari, S., Mircea, M., Giulianelli, L., Finessi, E., Rinaldi, M., Fuzzi, S., Marinoni, A., Duchi, R., Perrino, C., Sargolini, T., Vardè, M., Sprovieri, F., Gobbi, G. P., Angelini, F., Facchini, M.C., 2010. Size-resolved aerosol chemical composition over the Italian Peninsula during typical summer and winter conditions. Atmos. Environ. 44 (39), 5269–5278. https://doi.org/10.1016/j.atmosenv.2010.08.008.

Cesari, D., Genga, A., Ielpo, P., Siciliano, M., Mascolo, G., Grasso, F.M., Contini, D., 2014. Source apportionment of PM2.5 in the harbour–industrial area of Brindisi (Italy): identification and estimation of the contribution of in-port ship emissions. Sci. Total Environ. 497–498, 392–400. https://doi.org/10.1016/j.scitotenv.2014.08.007.

Cesari, D., Merico, E., Grasso, F.M., Dinoi, A., Conte, M., Genga, A., Siciliano, M., Petralia, E., Stracquadanio, M., Contini, D., 2021. Analysis of the contribution to PM10 concentrations of the largest coal-fired power plant of Italy in four different sites. Atmos. Pollut. Res. 12, 101135.

Chianese, E., Tirimberio, G., Riccio, A., 2019. PM2.5 and PM10 in the urban area of Naples: chemical composition, chemical properties and influence of air masses origin. J. Atmos. Chem. 76, 151–169. https://doi.org/10.1007/s10874-019-09392-3.

Chow, J.C., Lowenthal, D.H., Chen, L.-W.A., Wang, X., Watson, J.-G., 2015. Mass reconstruction methods for PM2.5: a review. Air Qual. Atmos. Health 8, 243–263. https://doi.org/10.1007/s11869-015-0338-3.

Contini, D., Merico, E., 2021. Recent advances in studying air quality and health effects of shipping emissions. Atmosphere 12, 92. https://doi.org/10.3390/atmos12010092.

Contini, D., Genga, A., Cesari, D., Siciliano, M., Donateo, A., Bove, M.C., Guascito, M.R., 2010. Characterisation and source apportionment of PM10 in an urban background site in Lecce. Atmos. Res. 95, 40–54.

Corbin, J.C., Pieber, S.M., Czech, H., Zanatta, M., Jakobi, G., Massabò, D., Orasche, J., El Haddad, I., Mensah, A.A., Stengel, B., Drinovec, L., Mocnik, G., Zimmermann, R., Prévôt, A.S.H., Gysel, M., 2018. Brown and black carbon emitted by a marine engine operated on heavy fuel oil and distillate fuels: Optical properties, size distributions, and emission factors. J. Geophys. Res. Atmos. 123, 6175–6195. https://doi.org/10.1029/2017JD027818.

Corsini, E., Marinovich, M., Vecchi, R., 2019. Ultrafine particles from residential biomass combustion: a review on experimental data and toxicological response. Int. J. Mol. Sci. 20, 4992. https://doi.org/10.3390/ijms20204992.

Crocchianti, S., Del Sarto, S., Ranalli, M.G., Moroni, B., Castellini, S., Petroselli, C., Cappelletti, D., 2021. Spatiotemporal correlation of urban pollutants by long-term measurements on a mobile observation platform. Environ. Pollut. 268, 115645.

Cuccia, E., Bernardoni, V., Massabò, D., Prati, P., Valli, G., Vecchi, R., 2010. An alternative way to determine the size distribution of airborne particulate matter. Atmos. Environ. 44, 3304–3313. https://doi.org/10.1016/j.atmosenv.2010.05.045.

Daellenbach, K.R., Manousakas, M., Jiang, J., Cui, T., Chen, Y., El Haddad, I., Fermo, P., Colombi, C., Prèvot, A.S.H., 2023. Organic aerosol sources in the Milan metropolitan area – receptor modelling based on field observations and air quality modelling. Atmos. Environ. 307, 119799 https://doi.org/10.1016/j.atmosenv.2023.119799.

D'Alessandro, A., Lucarelli, F., Mando, P.A., Marcazzan, G., Nava, S., Prati, P., Valli, G., Vecchi, R., Zucchiatti, A., 2003. Hourly elemental composition and sources identification of fine and coarse PM10 particulate matter in four Italian towns. J. Aeros. Sci. 34, 243–259. https://doi.org/10.1016/S0021-8502(02)00172-6.

Diana, A., Bertinetti, S., Abollino, O., Giacomino, A., Buoso, S., Favilli, L., Inaudi, P., Malandrino, M., 2023. PM10 element distribution and environmental-sanitary risk analysis in two Italian industrial cities. Atmosphere 14 (1), 48. https://doi.org/10.3390/atmos14010048.

Eurostat, 2022a. https://european-union.europa.eu/principles-countries-history/key-facts-and-figures/life-eu_en.

Eurostat, 2022b. https://ec.europa.eu/eurostat/web/structural-business-statistics/information-on-data/business-demography.

Fang, T., Lakey, P.S.J., Weber, R.J., Shiraiwa, M., 2019. Oxidative potential of particulate matter and generation of reactive oxygen species in epithelial lining fluid. Environ. Sci. Technol. 53, 12784–12792. https://doi.org/10.1021/acs.est.9b03823.

Ferrero, L., Castelli, M., Ferrini, B.S., Moscatelli, M., Perrone, M.G., Sangiorgi, G., Rovelli, G., D'Angelo, L., Moroni, B., Scardazza, F., Mocnik, G., Bolzacchini, E., Petitta, M., Cappelletti, D., 2014. Impact of black carbon aerosol over Italian basin valleys: high resolution measurements along vertical profiles, radiative forcing and heating rate. Atmos. Chem. Phys. 9641–9664.

Grau-Bové, J., Strlič, M., 2013. Fine particulate matter in indoor cultural heritage: a literature review. Herit. Sci. 1, 8. https://doi.org/10.1186/2050-7445-1-8.

Harrison, X.A., Donaldson, L., Correa-Cano, M.E., Evans, J., Fisher, D.N., Goodwin, C.E. D., Robinson, B.S., Hodgson, D.J., Inger, R., 2018. A brief introduction to mixed effects modelling and multi-model inference in ecology. PeerJ 6, e4794. https://doi.org/10.7717/peerj.4794.

Ielpo, P., Placentino, C.M., Cafagna, I., de Gennaro, G., Amodio, M., Daresta, B.E., Di Gilio, A., 2011. Role of the ionic component and carbon fractions in the fine and coarse fractions of particulate matter for the identification of pollution sources: application of receptor models. In: InTech (Ed.), Air Quality Monitoring, Assessment and Management. https://doi.org/10.5772/16723.

Isprambiente, 2011. https://www.isprambiente.gov.it/files/pubblicazioni/statoambiente/tematiche2011.

Istat, De Panizza, Andrea, Salomone, Alda, Faramondi, Alessandro, Franconi, Luisa, Quattrociocchi, Luciana (Eds.), 2020. Rapporto sul Territorio 2020. Ambiente Economia e Società. Istat - Istituto Nazionale di Statistica. https://doi.org/10.1481/Istat.RapportoTerritorio.2020. ISBN: 978-88-458-2014-4. in Italian.

Istat, 2023. https://demo.Istat.it/?l=en.

Kim, E., Hopke, P.K., Edgerton, E.S., 2003. Source identification of Atlanta aerosol by positive matrix factorization. J. Air Waste Manage. Assoc. 53 (6), 731–739. https://doi.org/10.1080/10473289.2003.10466209.

Kinney, P.L., 2018. Interactions of climate change, air pollution, and human health. Curr. Environ. Health Rpt. 5, 179–186. https://doi.org/10.1007/s40572-018-0188-x.

Krumbein, W., Gorbushina, A., 2009. Some aspects of biological weathering and air pollution. In: Hamilton, R., Kucera, V., Tidblad, J., Watt, J. (Eds.), The Effects of Air Pollution on Cultural Heritage. Springer, Boston, MA. https://doi.org/10.1007/978-0-387-84893-8_5.

Li, X., Ye, Y., Li, M.J., Ng, M.K., 2010. On cluster tree for nested and multi-density data clustering. Pattern Recogn. 43 (9), 3130–3143. https://doi.org/10.1016/j.patcog.2010.03.020.

Li, L., Lurmann, F., Habre, R., Urman, R., Rappaport, E., Ritz, B., Chen, J.-C., Gillil, F.D., Wu, J., 2017. Constrained mixed-effect models with ensemble learning for prediction of nitrogen oxides concentrations at high spatiotemporal resolution. Environ. Sci. Technol. 51 (17), 9920–9929. https://doi.org/10.1021/acs.est.7b01864.

Masiol, M., Rampazzo, G., Ceccato, D., Squizzato, S., Pavoni, B., 2010. Characterization of PM10 sources in a coastal area near Venice (Italy): an application of factor-cluster analysis. Chemosphere 80, 771–778. https://doi.org/10.1016/j.chemosphere.2010.05.008.

Masiol, M., Squizzato, S., Ceccato, D., Rampazzo, G., Pavoni, B., 2012. Determining the influence of different atmospheric circulation patterns on PM10 chemical composition in a source apportionment study. Atmos. Environ. 63 (2012), 117–124.

Masiol, M., Squizzato, S., Formenton, G., Khan, M.B., Hopke, P.K., Nenes, A., Pandis, S. N., Tositti, L., Benetello, F., Visin, F., Pavoni, B., 2020. Hybrid multiple-site mass closure and source apportionment of PM2.5 and aerosol acidity at major cities in the Po Valley. Sci. Total Environ. 704, 135287.

Massimi, L., Ristorini, M., Eusebio, M., Florendo, D., Adeyemo, A., Brugnoli, D., Canepari, S., 2017. Monitoring and evaluation of Terni (Central Italy) air quality through spatially resolved analyses. Atmosphere 8, 200.

Merico, E., Cesari, D., Gregoris, E., Gambaro, A., Cordella, M., Contini, D., 2021. Shipping and air quality in Italian port cities: state-of-the-art analysis of available results of estimated impacts. Atmosphere 12, 536. https://doi.org/10.3390/atmos12050536.

Mikkonen, S., Korhonen, H., Romakkaniemi, S., Smith, J.N., Joutsensaari, J., Lehtinen, K. E.J., Hamed, A., Breider, T.J., Birmili, W., Spindler, G., Plass-Duelmer, C., Facchini, M.C., Laaksonen, A., 2011. Meteorological and trace gas factors affecting

the number concentration of atmospheric Aitken (D_p = 50 nm) particles in the continental boundary layer: parameterization using a multivariate mixed effects model. Geosci. Model Dev. 4, 1–13. https://doi.org/10.5194/gmd-4-1-2011.

Moroni, B., Cappelletti, D., Marmottini, F., Scardazza, F., Ferrero, L., Bolzacchini, E., 2012. Integrated single particle-bulk chemical approach for the characterization of local and long-range sources of particulate pollutants. Atmos. Environ. 50, 267–277.

Nagl, C., Spangl, W., Buxbaum, I., 2019. Sampling points for air quality. In: Study for the Committee on the Environment, Public Health and Food Safety, Policy Department for Economic. Scientific and Quality of Life Policies, European Parliament, Luxembourg.

Nava, S., Calzolai, G., Chiari, M., Giannoni, M., Giardi, F., Becagli, S., Severi, M., Traversi, R., Lucarelli, F., 2020. Source apportionment of PM2.5 in Florence (Italy) by PMF analysis of aerosol composition records. Atmosphere 11, 484. https://doi.org/10.3390/atmos11050484.

Norris, G., Duvall, R., Brown, S., Bai, S., 2014. EPA Positive Matrix Factorization (PMF) 5.0 Fundamentals and User Guide. EPA/600/R-14/108. www.epa.gov.

OECD, 2021. Urban population by city size - OECD Data. https://data.oecd.org/popregion/urban-population-by-city-size.htm.

Paatero, P., 1999. The multilinear engine – a table-drive least squares program for solving multilinear problems, including the n-way parallel factor analysis model. J. Comput. Graph. Stat. 8 (4), 854–888. https://doi.org/10.1080/10618600.1999.10474853.

Paatero, P., Tapper, U., 1994. Positive matrix factorization: a non-negative factor model with optimal utilisation of error estimates of data values. Environmetrics 5, 111–126. https://doi.org/10.1002/env.3170050203.

Paatero, P., Eberly, S., Brown, S.G., Norris, G.A., 2014. Methods for estimating uncertainty in factor analytic solutions. Atmos. Meas. Tech. 7, 781–797. https://doi.org/10.5194/amt-7-781-2014.

Padoan, E., Malandrino, M., Giacomino, A., Grosa, M.M., Lollobrigida, F., Martini, S., Abollino, O., 2016. Spatial distribution and potential sources of trace elements in PM10 monitored in urban and rural sites of Piedmont Region. Chemosphere 145, 495–507. https://doi.org/10.1016/j.chemosphere.2015.11.094.

Park, M., Joo, H.S., Lee, K., Jang, M., Kim, S.D., Kim, I., Borlaza, L.J.S., Lim, H., Shin, H., Chung, K.H., Choi, Y.-H., Park, S.G., Bae, M.-S., Lee, J., Song, H., Park, K., 2018. Differential toxicities of fine particulate matters from various sources. Sci. Rep. 8, 17007. https://doi.org/10.1038/s41598-018-35398-0.

Pernigotti, D., Belis, C.A., Spano, L., 2016. SPECIEUROPE: the European data base for PM source profiles. Atmos. Pollut. Res. 7 (2), 307–314. http://source-apportionment.jrc.ec.europa.eu/specieurope/index.aspx.

Perrino, C., Catrambone, M., Di Menno Di Bucchianico, A., Allegrini, I., 2002. Gaseous ammonia in the urban area of Rome, Italy and its relationship with traffic emissions. Atmos. Environ. 36 (34), 5385–5394. https://doi.org/10.1016/S1352-2310(02)00469-7.

Perrino, C., Canepari, S., Cardarelli, E., Catrambone, M., Sargolini, T., 2008. Inorganic constituents of urban air pollution in the Lazio region (Central Italy). Environ. Monit. Assess. 136, 69–86. https://doi.org/10.1007/s10661-007-9718-y.

Perrino, C., Catrambone, M., Dalla Torre, S., Rantica, E., Sargolini, T., Canepari, S., 2014. Seasonal variations in the chemical composition of particulate matter: a case study in the Po Valley. Part I: macro-components and mass closure. Environ. Sci. Pollut. Res. 21 (6), 3999–4009.

Pey, J., Perez, N., Cortes, J., Alastuey, A., Querol, X., 2013. Chemical fingerprint and impact of shipping emissions over a western Mediterranean metropolis: primary and aged contributions. Sci. Total Environ. 463, 497–507. https://doi.org/10.1016/j.scitotenv.2013.06.061.

Pietrodangelo, A., Salzano, R., Rantica, E., Perrino, C., 2013. Characterisation of the local topsoil contribution to airborne particulate matter in the area of Rome (Italy). Source profiles. Atmos. Environ. 69, 1–14. https://doi.org/10.1016/j.atmosenv.2012.11.059.

Pio, Casimiro, Cerqueira, Mário, Harrison, Roy M., Nunes, Teresa, Mirante, Fátima, Alves, Célia, Oliveira, César, Sanchez, Ana, de la Campa, Begoña, Artíñano, Manuel Matos, 2011. OC/EC ratio observations in Europe: re-thinking the approach for apportionment between primary and secondary organic carbon. Atmos. Environ. 45 (34) https://doi.org/10.1016/j.atmosenv.2011.08.045.

Pio, C., Casotti Rienda, I., Nunes, T., Gonçalves, C., Tchepel, O., Pina, N.K., Rodrigues, J., Lucarelli, F., Alves, C., 2022. Impact of biomass burning and non-exhaust vehicle emissions on PM10 levels in a mid-size non-industrial western Iberian city. Atmos. Environ. 289, 119293 https://doi.org/10.1016/j.atmosenv.2022.119293.

PREPAIR Life15/IPE/IT/000013. Available at: https://www.lifeprepair.eu/index.php/azioni/air-quality-and-emission-evaluation/.

Sandrini, S., Fuzzi, S., Piazzalunga, A., Prati, P., Bonasoni P., Cavalli, F., Bove, M.C., Calvello, M., Cappelletti, D., Colombi, C., Contini, D., De Gennaro, G., Di Gilio, A., Fermo, P., Ferrero, L., Gianelle, V., Giugliano, M., Ielpo, P., Lonati, G., Marinoni, A … Gilardoni, S., 2014. Spatial and seasonal variability of carbonaceous aerosol across Italy. Atmos. Environ., 99, 587–598.

Scotto, F., Bacco, D., Lasagni, S., Trentini, A., Poluzzi, V., Vecchi, R., 2021. A multi-year source apportionment of PM2.5 at multiple sites in the southern Po Valley (Italy). Atmos. Pollut. Res. 12 (11), 101192 https://doi.org/10.1016/j.apr.2021.101192.

Seinfeld, J.H., Pandis, S.N., 2006. Atmospheric Chemistry and Physics: From Air Pollution to Climate Change, 2nd edition. John Wiley & Sons, New York.

Sun, H., Wang, S., Jiang, Q., 2004. FCM-based model selection algorithms for determining the number of clusters. Pattern Recognit. 37 (10), 2027–2037. https://doi.org/10.1016/j.patcog.2004.03.012.

Tositti, L., Brattich, E., Masiol, M., Baldacci, D., Ceccato, D., Parmeggiani, S., Stracquadanio, M., Zappoli, S., 2014. Source apportionment of particulate matter in a large city of southeastern Po Valley (Bologna, Italy). Environ. Sci. Pollut. Res. 21, 872–890. https://doi.org/10.1007/s11356-013-1911-7.

Tositti, L., Morozzi, P., Brattich, E., Zappi, A., Calvello, M., Esposito, F., Lettino, A., Pavese, G., Sabia, S., Speranza, A., Summa, V., Caggiano, R., 2022. Apportioning PM1 in a contrasting receptor site in the Mediterranean region: aerosol sources with an updated sulfur speciation. Sci. Total Environ. 851 (1), 158127 https://doi.org/10.1016/j.scitotenv.2022.158127.

Traversi, R., Becagli, S., Calzolai, G., Chiari, M., Giannoni, M., Lucarelli, F., Nava, S., Rugi, F., Severi, M., Udisti, R., 2014. A comparison between PIXE and ICP-AES measurements of metals in aerosol particulate collected in urban and marine sites in Italy. Nucl. Instr. Meth. Phys. Res. B 318, 130–134. https://doi.org/10.1016/j.nimb.2013.05.102.

Tuet, W.Y., Liu, F., de Oliveira Alves, N., Fok, S., Artaxo, P., Vasconcellos, P., Champion, J.A., Ng, N.L., 2019. Chemical oxidative potential and cellular oxidative stress from open biomass burning aerosol. Environ. Sci. Technol. Lett. 6, 126–132. https://doi.org/10.1021/acs.estlett.9b00060.

Vassura, I., Venturini, E., Marchetti, S., Piazzalunga, A., Bernardi, E., Fermo, P., Passarini, F., 2014. Markers and influence of open biomass burning on atmospheric particulate size and composition during a major bonfire event. Atmos. Environ. 82, 218–225. https://doi.org/10.1016/j.atmosenv.2013.10.037.

Vecchi, R., Bernardoni, V., Valentini, S., Piazzalunga, A., Fermo, P., Valli, G., 2018. Assessment of light extinction at a European polluted urban area during wintertime: impact of PM1 composition and sources. Environ. Pollut. 233, 679–689. https://doi.org/10.1016/j.envpol.2017.10.059.

Viana, M., Kuhlbusch, T.A.J., Querol, X., Alastuey, A., Harrison, R.M., Hopke, P.K., Winiwarter, W., Vallius, M., Szidat, S., Prévôt, A.S.H., Hueglin, C., Bloemen, H., Wåhlin, P., Vecchi, R., Miranda, A.I., Kasper-Giebl, A., Maenhaut, W., Hitzenberger, R., 2008. Source apportionment of particulate matter in Europe: a review of methods and results. J. Aero Sci. 39, 827–849 (DOI:j.jaerosci.2008.05.007).

Vidović, K., Hočevar, S., Menart, E., Drventić, I., Grgić, I., Kroflič, A., 2022. Impact of air pollution on outdoor cultural heritage objects and decoding the role of particulate matter: a critical review. Environ. Sci. Pollut. Res. 29, 46405–46437. https://doi.org/10.1007/s11356-022-20309-8.

Yttri, K.E., Simpson, D., Bergström, R., Kiss, G., Szidat, S., Ceburnis, D., Eckhardt, S., Hueglin, C., Nøjgaard, J.K., Perrino, C., Pisso, I., Prevot, A.S.H., Putaud, J.-P., Spindler, G., Vana, M., Zhang, Y.-L., Aas, W., 2019. The EMEP intensive measurement period campaign, 2008–2009: characterizing carbonaceous aerosol at nine rural sites in Europe. Atmos. Chem. Phys. 19, 4211–4233. https://doi.org/10.5194/acp-19-4211-2019.

Zhao, J., Zhang, Y., Xu, H., Tao, S., Wang, R., Yu, Q., Chen, Y., Zou, Z., Ma, W., 2021. Trace elements from ocean-going vessels in East Asia: vanadium and nickel emissions and their impacts on air quality. J. Geophys. Res. Atmos. 126, 8 https://doi.org/10.1029/2020JD033984 e2020JD033984.